EVALUATION OF SMALL UNILAMELLAR VESICLES AS A REMOVAL METHOD OF BENZO[A]PYRENE FROM HUMIC SUBSTANCES IN SOILS

A Thesis
Submitted to
the Temple University Graduate Board

In Partial Fulfillment
of the Requirements for the Degree
MASTER OF SCIENCE

---

by
Alexis A. Nawotka
May 2019

Thesis Approvals:

Dr. Bojeong Kim, Thesis Advisor, Earth and Environmental Science
Dr. David Grandstaff, Earth and Environmental Science
Dr. Steven Chemtob, Earth and Environmental Science

ABSTRACT

Polycyclic aromatic hydrocarbons (PAHs) are highly hydrophobic and lipophilic and are readily retained by soil surfaces and organic matter. Hence, several techniques have been developed in an effort to economically and effectively remove them from soil solids. Their strong affinity to soil organic matter limits their biodegradation processes by microorganisms, making them persistent in the soil environment. Recently, the use of "small unilamellar vesicles" (SUVs), nano-scale lipid aggregates, has been proposed as a means to enhance these microbial degradations, by effectively solubilizing lipophilic PAHs from the soil solids. In this thesis, laboratory-scale batch experiments were performed to examine this potential by measuring the uptake of benzo[a]pyrene (BaP), a model PAH compound, by SUVs from a simulated soil organic matter. This environmental surface was created by coating silica (SiO_2) nanospheres with a layer of poly-L-lysine, followed by humic acid, and characterized by dynamic light scattering for particle size and zeta potential values. Then, these humic acid-bound SiO_2 particles were saturated with BaP and then equilibrated with SUVs. The uptake of BaP by SUVs was measured through fluorescence spectroscopy, and the average amount of BaP concentrated in the 1 mg/L humic acid-bound SiO_2 particles was found to be 1.77 µg/L. After one week of equilibration with SUVs, 94.4% and 83.6% of the added BaP was solubilized by SUVs (in solutions containing 50 mg/L and 100 mg/L of vesicles, respectively), indicating an excellent ability to extract BaP from the soil organic particles. SUVs can therefore be an effective vehicle to enhance the biodegradability of PAHs in soils, with potential as an environmentally sustainable and affordable method.

ACKNOWLEDGMENTS

I would like to thank my thesis advisor most especially, Dr. Bojeong Kim, for guiding me through my return to academia, providing endless help for issues related to research and writing, and for having patience with me throughout. I would also like to thank my committee members, Dr. Grandstaff and Dr. Chemtob, for their help and teaching, and the partial use of their laboratories in the process of research, and Shelah Cox in administration, for always being positive and supportive and helpful with paperwork. I am indebted to Dr. Stephanie Wunder and her graduate students, including Sanaz Bandegi, Jordan Aguirre, and Prasanthy Garlapati. This group helped me with instrumental training and synthesis procedures, and was always cheerful and welcoming even when I showed up with another problem in hand. I would like to thank the other graduate students in EES for their support and assistance, and my family for holding me up throughout the entire process. This research was financially made possible by the Graduate Research Award Sustainability Program (GRASP), awarded by the Temple University Office of Sustainability.

TABLE OF CONTENTS

Page

LIST OF TABLES

Table Page

LIST OF FIGURES

CHAPTER ONE

INTRODUCTION

Humic substances are the largest constituent of soil organic matter (approximately 60%) which are produced through the chemical and biological decay processes of dead plant or animal materials, via progressive oxidation and enzymatic breakdown (Perminova and Hatfield, 2005). Humic substances can be further defined as humin, humic acids, and fulvic acids, where each one is distinguished from the others on the basis of their molecular weights and their solubility as a function of pH (MacCarthy, 2001a). Both of these acids have the same chain-ending functional groups, such as phenols, alcohols, and carboxylic acid groups, in varying proportions (MacCarthy, 2001a). Humic acid generally possesses longer chains and more complex structure, and shows a tendency towards fewer functional groups containing oxygen (Tang et al., 2014). Representations of humic and fulvic acids are given in figure 1.1.

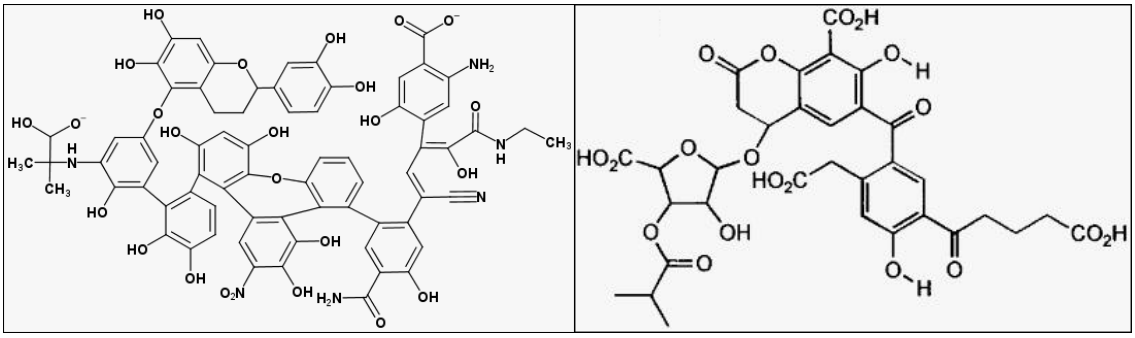

Figure 1.1. Representative structure for humic acid (left), after Perminova and Hatfield (2005, Figure 1), and fulvic acid (right), after MacCarthy (2001a, Figure 1). Average weights are 2000 Da for humic acids, and 700 Da for fulvic acids (MacCarthy, 2001a).

Due to the presence of multiple functional groups, humic materials can interact with metal ions and organic compounds, primarily through ion exchange, complexation, and redox reactions (Perminova and Hatfield, 2005). Therefore, when a spill of a hazardous chemical or contaminant occurs, these reactions control the fate and behavior of metals and organic compounds in the terrestrial environment. These interactions are influenced by the nature of the contaminant, and by geochemical conditions including groundwater pH and concentration gradients (Perelo, 2010).

In addition, for spills, the scale of the contamination site and the availability of financial resources for cleanup are of critical importance. Hazardous spills may fall under government oversight as part of the Comprehensive Environmental Response, Compensation, and Liability Act (2012) enacted in 1980, commonly referred to as the "Superfund" program; several former or active sites in this program exemplify the difficulties noted here. For instance, the Drake Chemical site in Lock Haven, PA, was the site of a plant which formerly manufactured chemicals used for dyeing and rubber production and had served this purpose for other companies before Drake Chemical acquired the site in 1962 (Martin, 1998). A primary contaminant of concern was 2-naphthylamine, a hydrocarbon and carcinogen which sorbs strongly onto soil solids; site contamination was extensive in scope, and disposal costs for 2-naphthylamine were declared to be $140 million (Martin, 1998). Another site, the Metal Bank site in Philadelphia, PA, previously recovered copper from electrical transformers and kept the waste transformer oil in underground storage tanks (U.S. Environmental Protection Agency, 2018). These tanks leaked oil into the groundwater and subsequently into the Delaware River. Nearby riverbank sediments tested positively for polychlorinated

biphenyls (PCBs), a primary component of transformer oil (U.S. EPA, 2018). While the final cost of the project was not disclosed by the Environmental Protection Agency (EPA), this extensive release into the environment made the parties responsible for the site, Union Corporation and Metal Bank of America, file for bankruptcy 11 months after the declaration (U.S. EPA, 2018).

Remediation sites such as the Drake Chemical and Metal Bank sites require carefully planned and costly projects. The method selected for cleanup of the site, therefore, is critically important and should minimize expenses, while covering the maximum possible extent with effectiveness in removal of a target contaminant. Most of the techniques for removal of chemical contaminants have required specialized equipment or extensive periods of time, including chemical oxidation or reduction, electrochemical reduction, and phytoremediation (Siegrist et al., 2011). Additionally, *in situ* flushing with surfactant chemicals, electrochemical mobilization of contaminants, and *ex situ* polymer-based extraction have been used to remediate soils or sediments (Mulligan et al., 2001; Gómez et al., 2009; Mosca Angelucci and Tomei, 2015). A summary of the advantages and disadvantages of these methods is given in Table 1.1.

Table 1.1

Summary of Several Environmental Remediation Methods

Method	Advantages	Disadvantages
Chemical oxidation/reduction[1,2]	Effective with polycyclic aromatic hydrocarbons (PAHs); Many treatment methods are effective; Oxidation treatment enhances bioremediation	Can require tight control of subsurface pH; Concern about fate of chemicals used in treatment; Potentially hazardous degradation by-products
Electrochemical reduction[3]	Treats for both metals and organics; *In situ* or *ex situ*; Saturated or unsaturated	Requires significant understanding of local geochemistry
Phytoremediation[4]	Uses vegetation as active agent, seen as environmentally friendly; Low cost	May require much time; Not effective for deeply placed contaminants
Surfactant flushing[5]	Facilitates desorption and biodegradation of very hydrophobic species; Naturally occurring biosurfactants are effective	Synthetic surfactants may be toxic, sorb to soil, and resist biodegradation
Electrochemical mobilization[6]	Treats for both organic and inorganic species; Effective in soil of low hydraulic conductivity	May require surfactant or co-solvent; Slow treatment; Less effective for contaminants with lower aqueous solubilities
Polymer-based extraction[7]	Has high removal efficiency for certain contaminants; Rapid treatment time	Usually done *ex situ*; Efficacy controlled by level of soil moisture and of contamination, and polymer type

[1]Tsai et al., 2011.
[2]Ferrarese et al., 2008.
[3]Reddy and Cameselle, 2009.
[4]Nyer, 2001, Ch. 9.
[5]Pei et al., 2017.
[6]Gómez et al., 2009.
[7]Tomei et al., 2015.

In recent years, considerable attention has been devoted to the application of nano-sized (1-100 nanometers) materials for environmental remediation. For instance, nano-scale zero-valent iron (ZVI) has been shown to be effective in the degradation of contaminants such as PCBs, organochlorine pesticides, and organic dyes, *in situ* through chemical reduction by ZVI or adsorption to ZVI particles (Zhang and Elliott, 2006). However, caution is still advised when using ZVI for remediation of organic contaminants with regard to the ultimate fate of the particles in the environment and their ecotoxicity, as well as the standardization of eco-friendly particle production methods. For instance, limited mobility (several meters or less) of uncoated ZVI particles was observed in field-scale trials, primarily due to aggregation and oxidation of particle surfaces, causing clogging of pore spaces and limiting their delivery through soil profiles (Crane and Scott, 2012). Coating the particles with polyelectrolyte compounds greatly improves mobility; however, the persistence of the coating material may raise other environmental problems (Crane and Scott, 2012).

Additionally, the electrochemical reduction of organic contaminants by ZVI produces Fe^{2+} and Fe^{3+} ions and consumes protons, and may increase soil solution pH (Crane and Scott, 2012). For the production of the particles, the use of sodium borohydride is required for reduction of iron to Fe^{0}, producing H_2 gas and creating a disposal problem with excess toxic $NaBH_4$ (Machado et al., 2013). Due to aforementioned concerns with ZVI methods, effort has been directed to further explore the properties and usefulness of other nano-materials, such as monometallic and bimetallic particles (silver, copper, iron/nickel and iron/palladium), titanium dioxide and zinc oxide, gold, fullerenes, carbon nanotubes, and lipid-based particles. In particular,

lipid-based materials demonstrate the ability to sequester and transport hydrophobic compounds and are inexpensive to produce; both lipid-based and ZVI particles also share ease of transport in the porous environment media (Machado et al., 2013; Wang et al., 2015). This thesis will focus on lipid-based materials, namely small unilamellar vesicles (SUVs), approximately 100 nanometers in size, and examine their properties and potential to sequester benzo[a]pyrene (BaP, structure shown in figure 1.2) acting as a model contaminant.

1.1 Compositions and Properties of Humic Substances

Although humic substances are mixtures of humin, humic acids, and fulvic acids (Perminova and Hatfield, 2005), the separation of humic acid from humin and fulvic acids is feasible due to differences in their solubility. Detailed methods can be found later in this thesis (Chapter 2, Methods). In general, humin is operationally defined as material which is insoluble across the entire pH range; humic acids are soluble only at high pH, greater than approximately 10, whereas fulvic acids are soluble across the entire pH range (Perminova and Hatfield, 2005).

Humic substances do not have any regular repeating unit in the structure and are not true polymers, although molecular weights may be potentially greater than 2000 Da. The structure may be more appropriately described as macromolecular (MacCarthy, 2001a). This recognition acknowledges the many different structural moieties that have been found in humic materials. Representative structures of humic and fulvic acids (Figure 1.1) show the presence of aromatic and aliphatic components, carboxylic acid, ketone groups, and ether linkages, amongst other features. The carboxylic acid and

phenol groups possess a weakly acidic character, primarily responsible for the ion-exchange reactions and complexation abilities of the acid. Aromatic and aliphatic moieties are responsible for hydrophobic character. The carboxylic acid groups also control interactions with mineral surfaces, and may react with dissolved species in solution (MacCarthy, 2001b).

Humic materials also possess a "refractory" nature; that is, mature humus is resistant to break down. This slowness or limitation in the degradation processes has been linked to the heterogeneity of the material (Stevenson, 1994, Ch. 2). Specifically, microbial degradation of an organic material requires enzyme activity, and typically, individual types of enzymes facilitate only one or two reactions. For example, the enzyme monophenol monooxygenase initiates the oxidative degradation of phenol compounds (Gramss et al., 1999). However, moieties and linkages in humus may form a wide variety of configurations (Stevenson, 1994, Ch. 2), adding complexity into the structure, and thus diminishing the efficacy of microbial enzymatic activities for break-down.

Attempts to isolate individual compounds from humic material have been made in the past but have been unsuccessful. MacCarthy (2001b) notes that after separation by one method, such as column chromatography or electrophoresis, the application of another method to any previous fraction results in further production of chemically different fractions. Further, separations proceed through multiple iterations, and continue to artificially produce new fractions. The problem may be described by stating that each molecule in humic material can be considered "unique", despite the commonality of properties amongst humic substances found in far-separated locations. Given the variety

of compounds that compose all humic substances, differentiating humic substances from non-humic substances becomes difficult: non-humic materials can include, for example, carbohydrates and amino acids in pristine and partially altered forms, more readily broken down than mature humic molecules (MacCarthy, 2001a).

Humic substances in the natural environment may be found suspended in groundwater, adsorbed to mineral particles and grains, or as aggregated particles within bulk soil (Joo et al., 2008). In particular, their adsorption onto mineral surfaces is facilitated by several mechanisms, such as anion exchange, hydrophobic interaction, and cation bridging, with the extent of adsorption primarily determined by the chemistry of the water and the functional groups on the humus particles (Joo et al., 2008). When sorbed and temporarily immobile, humic material may serve as an active surface for dissolved species at the soil-water interfaces. The present study is prompted by this recognition, i.e., humic materials are sorbed onto mineral grains in the environment, and is therefore accomplished by immobilizing humic acid onto silica nanospheres, with a well-controlled particle size of 100 nanometers in diameter, used as an analog of natural humic materials coated on mineral oxides. Silica was chosen as a mineral oxide in the present study, as it is an extremely common geomaterial on Earth's surface. Details of the humic acid immobilization for experiments can be found in a later section (Section 1.3) of this thesis.

1.2 Contaminants and their Interactions with Humic Materials

Soil contamination with heavy metals and/or organic compounds occurs through a wide variety of sources such as landfills, agricultural facilities, and industrial zones

(Wuana and Okieimen, 2011), affecting ecosystems and human health adversely. Organic chemicals can bind onto soil particles, and the co-presence of heavy metals often delays or hinders their breakdown by microbial activity (Wuana and Okieimen, 2011). In particular, the intermolecular interactions between humic material and organic contaminants are dependent on properties of the soil (e.g. pH, clay and humic material content) and the contaminant (e.g., hydrophobicity, acidity, and molecular size) (Haigh, 1996).

One particular class of organic chemicals, the polycyclic aromatic hydrocarbons (PAHs), are considered to be of high concern as they adsorb strongly to soil particles in this manner, and are known to be potential carcinogens or teratogens even at low concentrations (Garcia-Flores et al., 2016). PAHs can be introduced into the environment by combustion of carbonaceous matter or through oil or fuel spills (Walker, 2008, Ch. 9). PAHs in the atmosphere (e.g., ash from forest fires, or incomplete fossil fuel combustion) are eventually returned to the terrestrial environment through precipitation, via adsorption on airborne particulates (Walker, 2008, Ch. 9). Due to their high toxicity and persistence in the environment, PAH compounds are often used in studies to examine their environmental behaviors and fate, as well as to develop potential remediation methods for their clean up. All PAHs possess a backbone structure of two or more linked benzene rings, varying in number and the nature of the linkages, as can be seen in Figure 1.2.

Due to their backbones, most PAH compounds are entirely planar and possess no functional groups, presenting a high degree of hydrophobic character (Walker, 2008, Ch. 9). They can thus adsorb strongly to the hydrophobic residues and aliphatic components found in humic substances. However, not all PAHs sorb to the same extent. In order to

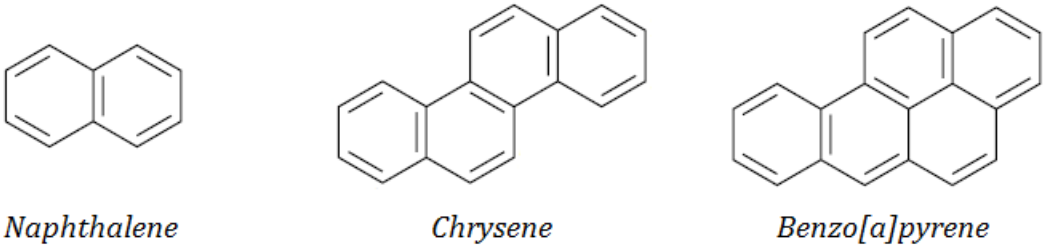

Figure 1.2. Examples of several polycyclic aromatic hydrocarbons (PAHs). Benzo[a]pyrene is the model PAH used in this work, and is carcinogenic (Garcia-Flores et al., 2016).

compare and contrast their relative hydrophobicity, the octanol-water coefficient (K_{ow}) can be used: the ratio of a compound's concentration in n-octanol phase to its concentration in water at equilibrium. Highly hydrophobic BaP (in figure 1.2) has a K_{ow} value of $10^{6.13}$ (De Maagd et al., 1998). In general, the higher the K_{ow} value of the compound, the stronger the sorption to soil particles. Therefore, the amount of hydrophobic contaminant that adsorbs on soil solids typically increases with the overall organic content of the soil (Haigh, 1996). This strong retention of the compound on soil solids makes it less available to microorganisms for potential degradation. Further, immobilized and concentrated organic contaminants, such as PAHs, can act as a temporary reservoir and continue to be a local source of PAHs in the environment (Haigh, 1996). While K_{ow} values differ under alternative experimental parameters, the water solubility of PAHs is generally low; for the compounds in figure 1.2, the Solubility Data Tables (published by the National Institute of Standards and Technology, NIST) list a value of 31 mg/L at 25°C for naphthalene, 1.5 μg/L at 27°C for chrysene, and 4.0 μg/L at 27°C for benzo[a]pyrene (Shaw et al., 2006a, 2006b). Due to this recalcitrance and the health hazard posed by these compounds, there has been much research into their

remediation, particularly with regard to their strong affinity for soil materials. Previous efforts with varying degrees of success have been summarized in Table 1.1 (Nyer, 2001; Reddy and Cameselle, 2009; Gómez et al., 2009; Tsai et al., 2011; Tomei et al., 2015; Pei et al., 2017). Using surfactants, in particular, for the removal of PAHs appears to be successful to some extent by effectively solubilizing them from soil solids (Mulligan et al., 2001; Lamichhane et al., 2017). This is accomplished by lipid compounds in the form of micelles, and several of these are named in the review paper by Lamichhane et al. (2017). Only a few studies have tested the potential of lipid bilayers as a removal vehicle of PAHs. Thus, this thesis aims to examine that potential by studying the interactions of humic acid-bound PAHs with lipid-based nanomaterials (i.e., lipid bilayers in section 1.4).

1.3 Immobilization of Humic Acid for Study

In order to better characterize the surface interactions between humic materials and PAHs, it is necessary to anchor the humic substances to a substrate. This provides a platform to carry out desired reactions and improves recovery of the material from laboratory batch reactions, and enables application of humic substances to routes of investigation such as high-performance liquid chromatography, so that compounds may be separated from each other on the basis of their interactions with humic acid (Ayyildiz, 2015). Humic acids in particular possess many different functional groups, several of which could potentially be utilized to anchor the humic acids to the substrate (Ayyildiz, 2015). For instance, zeolites mediated by cationic surfactants have been used for the attachment of humic acid (Lin et al., 2011). Specifically, zeolites possess a framework

silicate (tectosilicate) structure with an overall negative charge which is normally balanced by cations present in the environment, such as sodium and calcium. A surfactant, such as cetylpyridinium bromide, can be readily loaded onto the framework, displacing the cations through ion exchange, and the humic acids may then be immobilized by adsorption to the surfactant (Lin et al., 2011). This assembly is likely to be very effective in uptake of heavy metal ions, as the ions not only bind to the humic acids but also enter cation sites within the mineral framework where the surfactant molecules cannot enter (Lin et al., 2011). Zeolites are a suitable substrate as they are economically advantageous, and have high cation exchange capacities that allow large quantities of surfactant to sorb (Lin et al., 2011).

Humic acids have also been immobilized on cross-linked polystyrene resin and silica, of which there exist several functionalized derivatives (Koopal et al., 1998). Cross-linked polystyrene, although stable and able to be regenerated, was not suitable for production on a large scale, which would be required for use in remediation (Koopal et al., 1998). The use of silica as a substrate, however, has been extensively investigated, and humic acids have been bonded or adsorbed to silica with a variety of intermediaries. This interest is due in part to the environmental applicability of silica, to its chemical stability, and to its well-understood mechanical properties. Further, silica is a common material on the Earth's surface and is often found with humic acids in the natural environment, and it is stable over a reasonable range of pH values (Koopal et al., 1998). Many of the properties of silica, including surface area, particle size, and pore size, can be effectively controlled by experimental parameters (Koopal et al., 1998).

Functionalization of the silica surface before addition of humic acids has been accomplished with several intermediaries, including 3-aminopropyltrimethoxysilane, N,N-dimethylformamide, and glutaraldehyde (Koopal et al., 1998). Humic material can then be bonded directly to these compounds or adsorbed, and the attachment can be made through different functional groups. A widely-used preparation utilizes 3-aminopropyltrimethoxysilane as the intermediate between silica and humic acids, and these are known as "aminopropyl" silica preparations; however, this procedure requires curing time and is thus time-consuming (Koopal et al., 1998).

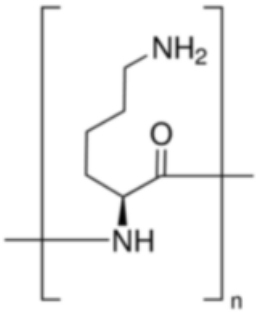

Figure 1.3. The structure of poly-L-lysine, a polymer and intermediary compound for bonding humic acid to a surface.

Therefore, this thesis utilizes a new preparation for adsorption of humic acids on silica mediated by poly-L-lysine polymer (Figure 1.3). This preparation method was originally developed for functionalization of bare silica surfaces for use in a quartz crystal microbalance (Chen and Elimelech, 2008), yet was never utilized for laboratory batch-scale experiments. The procedure is here adapted for preparation of the surfaces of silica nanoparticles which serve as the substrate for immobilization of humic acids.

1.4 Small Unilamellar Vesicles in PAH Remediation

Existing methods of soil remediation vary widely in scale, time commitment, and required resources (Table 1.1). For instance, *in situ* remediation may present considerable difficulties, as detailed characterization of the contaminated soil is required on a case-by-case basis. Infiltration of the soil with surfactants has shown promise in removal of organic contaminants, including solvents (Mulligan et al., 2001). Many different surfactants have been proposed or utilized in field study, including those injected as liquids such as saponin, Polysorbate 80, and alkyl polyglycoside (Pei et al., 2017), and those injected as foams, such as sodium dodecyl sulfate mixed with CO_2 (Maire et al., 2015). However, due to their potential toxicity to humans and organisms in the environment, as well as their degradability after use, using those surfactants requires caution (Mulligan et al., 2001).

Recently, the use of "nanoparticle-supported lipid bilayers" (NP-SLBs) has been proposed as an *in situ* remediation method for PAHs in the environment (Wang et al., 2015). NP-SLBs demonstrated enhanced colloidal stability and hence, greater mobility, while the lipid layer(s) could potentially sequester hydrocarbon contaminants such as BaP, acting effectively in remediating soil and sediment contamination (Wang et al., 2015). Due to natural abundance, silica was the choice of the core material for the NP-SLBs. These lipids may also exist without the solid core, in which case they are referred to as small unilamellar vesicles (SUVs) (Wang et al., 2015). Illustrations of these particles are presented in Figure 1.4. Details of the synthesis methods and characterization of NP-SLBs and SUVs can be found in Wang et al. (2015).

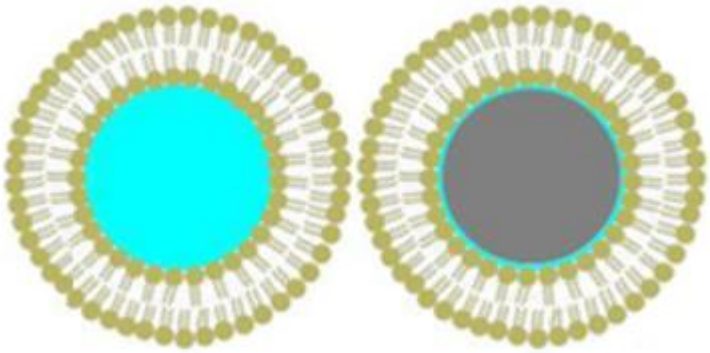

Figure 1.4. The structures of small unilamellar vesicles (left), and nanoparticle-supported lipid bilayers (right) with silica core. Lipid molecules are arranged in a spherical shape (modified after Wang et al., 2015, Figure 1).

Furthermore, Wang et al. (2015) have investigated the interactions of SUVs and NP-SLBs with humic acid, their ability to sorb BaP in the presence of humic acid, and their interactions with microorganisms, in order to consider the possibility of bacterial degradation and toxicity of the BaP extracted by SUVs and NP-SLBs. Those experiments were designed and performed to determine the applicability of the SUV system and NP-SLB system as remediation methods to treat soils contaminated with PAHs. Figure 1.5 illustrates the desorption of hydrocarbon contaminants from humic material due to a preferential sorption into the lipid bilayer structure.

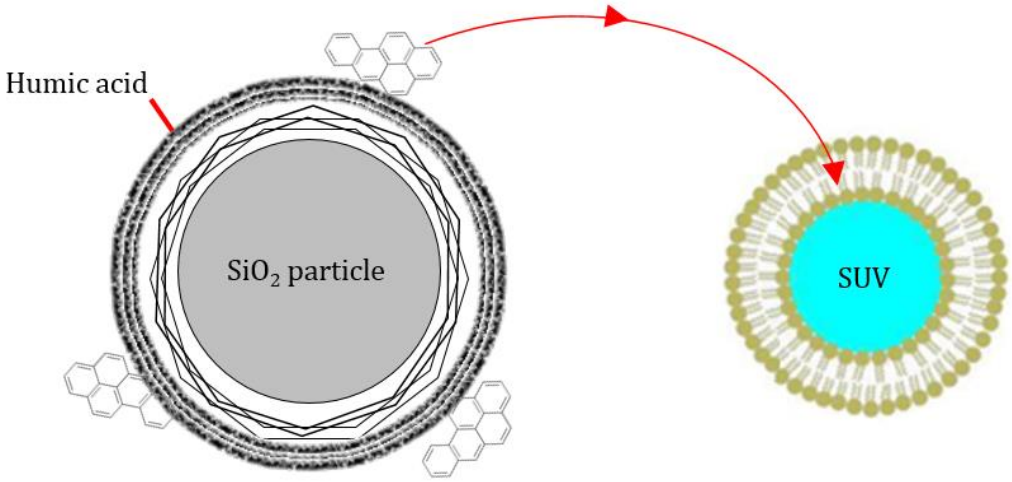

Figure 1.5. Desorption of benzo[a]pyrene from humic acid and sorption to SUVs. Structure of SUV modified after Wang et al. (2015, Figure 1).

However, humic acid in the experimental systems by Wang et al. (2015) was suspended in solution, unbound to any solid supports, representing dissolved organic matter. In soils, however, humic acid is frequently adsorbed to the surfaces of mineral grains and flakes, not suspended (Joo et al., 2008), and therefore humic acids bound on silica nanospheres, as described above in section 1.3 and shown in Figure 1.5, would better serve as a surrogate for natural organic matter in the environment. The present work starts with the synthesis of these silica-supported humic acid nanostructures to simulate a likely environmental scenario. The model organic contaminant, BaP, is strongly associated with the humic acid fraction of the silica-humic acid nanostructures. Then, this work expands to determine the efficacy of SUVs in extraction of BaP from the humic acid fraction, and thereby test its potential as a remediation method for BaP in the environment.

1.5 Hypotheses

1. Poly-L-lysine will serve as an effective agent to attach humic acids to silica nanospheres through adsorption, forming a layered composite nanoparticle.
2. Benzo[a]pyrene will preferentially be incorporated into small unilamellar vesicles over adsorption to humic acid, and this transfer may be quantitated by fluorescence spectroscopy.

CHAPTER TWO

MATERIALS AND METHODS

2.1 Materials

The humic acid (sodium salt, technical grade) was purchased from Aldrich Chemical Co., lot 01828JZ. A colloidal suspension of silicon dioxide spheres (Nissan Chemical Snowtex®, product code MP-1040H, lot 150117) was used as received, and diluted with deionized water to make a 5.05% wt solution. Poly-L-lysine (PLL, in hydrobromide form, lot SLBQ0620V) and benzo[a]pyrene (lot SLBF4553V) were purchased from Sigma-Aldrich. For the liposomes, 1,2-dimyristoyl-sn-glycero-3-phosphocholine (DMPC) was used from Avanti Polar Lipids, lot 850345-16-270. With the exception of humic acid (Aldrich Chemical Co.), no further purification was done on any reagent used in this experiment.

2.2 Purification of Humic Acid

Humic acid was purified prior to use by following the procedure described by Koopal et al. (1998). Five grams of humic acid were added to 500 mL of deionized water, previously adjusted to pH 11 with sodium hydroxide (Fisher Scientific), and stirred overnight at room temperature. This solution was centrifuged at 4,700 rpm for 30 minutes to remove undissolved material. The supernatant containing dissolved humic acid was then decanted and adjusted to a pH of 2 using 0.1 M HCl (Fisher Scientific), then stirred for 24 hours at room temperature to re-precipitate the humic acid. This solution was then

centrifuged at 10,000 rpm for 30 minutes and the supernatant discarded. The solid material was re-suspended in 0.01 M HCl, then stirred for two hours and centrifuged, and the supernatant was discarded; all of these steps were then repeated twice. After decanting the supernatant, the solid material was collected and allowed to dry overnight in a fume hood. The resultant black, glassy-looking solid was ground with a mortar and pestle for use in the following experiments.

2.3 Assembly of PLL- and Humic Acid-Coated Particles

The assembly of PLL and humic acid-coated SiO_2 particles was accomplished by modifying the experimental conditions originally proposed by Chen and Elimelech (2008). First, two milliliters of 5.05% wt SiO_2 solution, 0.2383 grams of HEPES buffer (Fisher Scientific) and 0.5844 grams of NaCl (EMD Millipore) were added to a 100 mL volumetric flask, which was filled with deionized water and mixed thoroughly. The resulting solution contained 1.3066 mg/mL of SiO_2, 10 mM HEPES, and 100 mM NaCl. For brevity, this solution is designated the "SiO_2 stock solution" for the rest of this thesis. A stock solution of PLL was also prepared in the same manner as the SiO_2 stock solution, by adding 10 mg of PLL to a total of 100 mL deionized water, making a 0.1 mg/mL PLL solution. This solution is designated the "PLL stock solution" for the rest of this thesis.

To determine the surface coverage of PLL on the SiO_2 particles, a series of solution mixtures was made by varying ratios of those two stock solutions. The size and zeta potential of the SiO_2 particles were then measured by dynamic light scattering (Malvern Zetasizer Nano ZSP). Note that in Table 2.1, the ratios are given by concentration with SiO_2 listed first, so that for the solution labeled "10:1", for example,

the concentration of SiO_2 spheres is ten times higher than that of PLL. At a given ratio, triplicated samples were prepared with the mixture of those stock solutions and individually analyzed as replicates.

Table 2.1

Volume of SiO_2 and PLL Stock Solutions Used to Produce Solution Mixtures with Varying Concentration Ratios

SiO_2:PLL Ratio	SiO_2 Stock (mL)	PLL Stock (mL)
1:5	0.2	10.0
1:2	0.5	10.0
1:1	0.5	5.0
1.43:1	0.5	3.5
2.50:1	1.0	4.0
10:1	1.0	1.0
20:1	2.0	1.0
30:1	3.0	1.0
40:1	4.0	1.0
50:1	5.0	1.0
60:1	3.0	0.5
70:1	3.5	0.5
80:1	4.0	0.5
90:1	4.5	0.5
100:1	10.0	1.0

Upon successful sorption of the PLL layer onto the silica nanospheres, purified humic acid was added to the assembled SiO_2:PLL particles. The humic acid solution was prepared by stirring 28.4 mg of purified, fine-ground humic acid in 52 mL of deionized water for two hours. The resulting solution was filtered through a 0.2 μm cellulose acetate filter (Whatman) to remove solids, and the filtrate was then adjusted to a pH of 5.5 with sodium hydroxide (Fisher Scientific).

The actual concentration of humic acid in this solution was not determined, as the focus was given to optimizing the volume ratio between the SiO_2/PLL and purified humic acid. The ratio of 50:1 (SiO_2: PLL) solution in Table 2.1 was chosen for the humic acid addition, as it contained the lowest amount of PLL while displaying a consistent particle size and zeta potential expected for PLL (Section 3.1.1). All following references in this section to "PLL-coated SiO_2" or "SiO_2/PLL" indicate this combination. Table 2.2 lists a range of volumes tested to optimize the experimental conditions; all ratios were tested in triplicate for particle size and zeta potential by dynamic light scattering (DLS), using a Malvern Zetasizer Nano ZSP.

Table 2.2

Volume Ratios of SiO_2/PLL and Humic Acid Solutions for the Assembly of Humic Acid-Coated Particles

Ratio	SiO_2/PLL (mL)	Humic Acid (mL)
1:6	6.0	36.0
1:5	6.0	30.0
1:4	6.0	24.0
1:3	6.0	18.0
1:2	18.0	36.0
1:1	3.0	3.0
2:1	3.0	1.5
3:1	3.0	1.0
4:1	3.0	0.75
5:1	3.0	0.60

A subset of ratios listed in Table 2.2, from 1:6 through 1:2, was centrifuged at 10,000 rpm for 30 minutes and the supernatant decanted, with the remaining solid allowed to dry in a fume hood overnight. When completely dry, these solids were

analyzed by thermogravimetric analysis (TA Instruments Hi-Res 2950), over a temperature range of 20°C to 800°C, to quantify the amount of humic acid adsorbed onto the PLL-coated SiO_2 nanospheres.

2.4 Preparation of Small Unilamellar Vesicles

Small unilamellar vesicles (SUVs) were prepared with DMPC and used as a component in both sample and standard solutions for analysis. Twenty milligrams of DMPC (Avanti Polar Lipids, lot 850345-16-270) were weighed into a glass vial and dissolved in approximately 3-4 mL of chloroform (JT Baker). This chloroform was then evaporated under a stream of nitrogen to produce a thin film on the bottom of the vial, and the vial was then placed under vacuum overnight.

The lipid film was then hydrated by adding 4 mL of deionized water and placing the vial into a warm water bath at approximately 40°C for twenty minutes. The temperature of the bath was not allowed to exceed 45°C at any time. The vial was then moved into a dry ice-acetone bath until the solution was frozen, allowed to sit for three to four minutes, then moved back into the 40°C water bath until the solution was fully thawed. This freeze-thaw cycle was repeated four more times, so that a total of five cycles were performed, and the end solution showed only cloudiness with no visible large particles.

The hydrated solution was then extruded into vesicles with an Avanti mini-extruder apparatus. This apparatus contains an inner chamber sealed by rubber O-rings, which contains a polycarbonate filter (Whatman Nucleopore 0.1 μm, lot 163090) and filter supports, and it is by repeated passage through the filter that the lipids are extruded

into liposomes. The apparatus was assembled and placed into a heating block maintained at 50°C. Two Hamilton 1000 μL gas-tight syringes were used for the extrusion, with one inserted into each end of the apparatus, and the hydrated lipid solution was passed back and forth between them 15-20 times, for a total of 30-40 plunger depressions. This resulting solution contained SUVs at 5 mg/mL, and additional quantities were prepared as needed throughout the experiment.

2.5 Preparation of Benzo[a]pyrene Standard Solutions

Three sets of standard solutions were prepared, one containing benzo[a]pyrene (BaP) only (1) and the other two containing BaP with different SUV concentrations (2).

(1) An initial stock solution was prepared by adding 10.0 mg of BaP to a 100 mL volumetric glass flask that contained approximately 70 mL of acetonitrile (Sigma-Aldrich), and mixing until BaP was fully dissolved. Then, additional acetonitrile was added up to 100 mL and mixed thoroughly. This 100 mg/L BaP stock solution was diluted to a 1 mg/L BaP solution with acetonitrile, and this 1 mg/L BaP solution was then used to prepare all the standards in the present study. The 100 mg/L and 1 mg/L BaP stock solutions were sealed tightly and stored in a refrigerator when not in use.

Then, 50, 40, 30, and 20 μL of 1 mg/L BaP stock solution were added into 10 mL of deionized water to make BaP standards of 5 μg/L through 2 μg/L respectively. A 1 μg/L standard was prepared by diluting the 2 μg/L standard with deionized water. These five BaP-only standards were prepared fresh on each day of use.

(2) Two sets of BaP standards were prepared with SUVs, one set with 50 mg/L (**SUV Standard Set 1**) and the other with 100 mg/L of vesicles (**SUV Standard Set 2**).

The original 5,000 mg/L solution of SUVs (section 2.4) was diluted to 1,000 mg/L with deionized water, and five vials were prepared by addition of 0.5 mL of this solution to 9.5 mL of deionized water. Each vial then contained 50 mg/L of SUVs in 10 mL of deionized water. Four standard solutions were made by adding 50, 40, 30, and 20 μL of 1 mg/L BaP stock to those vials. One standard was made by adding 100 μL of 0.1 mg/L BaP in acetonitrile to the last vial. The resulting five vials all contained 50 mg/L of SUVs, while BaP concentrations ran from 5 through 1 μg/L (**SUV Standard Set 1**). For the other standard set containing 100 mg/L SUVs, five vials were first prepared by adding 0.5 mL of 1000 mg/L SUV solution to 4.5 mL of deionized water, for a total volume of 5 mL. Then 150, 100, and 50 μL of 0.1 mg/L BaP in acetonitrile were added to those vials, creating the 3, 2, and 1 μg/L standards, respectively. In addition, 25 and 20 μL of 1 mg/L BaP in acetonitrile were added to the remaining two vials, creating the 5 and 4 μg/L standards, respectively. The resulting five vials all contained 100 mg/L of SUVs, while BaP concentrations ran from 5 through 1 μg/L (**SUV Standard Set 2**). SUV Standard Sets 1 and 2 were used to create calibration curves for BaP quantitation in the following experiment, and were tightly sealed and stored in a refrigerator when not in use.

2.6 Analysis of Benzo[a]pyrene on Humic Acid

A Photon Technology International (PTI) fluorimeter was used for the analysis of BaP and humic acid, using a pure quartz cuvette with a 10 mm path length. The instrument was run in "digital" hardware configuration, with a slit width of 5 nm for both excitation and emission monochromators. Step size was set to 1 nm and integration to 0.2 seconds, averaging one measurement per step. To find the optimal wavelengths for

analysis, multiple excitation and emission scans were run on a 1.0 mg/L humic acid solution (described later in this section) and on a 5 μg/L BaP solution (section 2.5), to find the highest response from BaP where the humic acid signature was negligible. It was thus determined to use an excitation wavelength of 362 nm and an emission wavelength of 405 nm for BaP; all quantification was made by calculating peak heights in collected spectra. The adsorption of BaP onto humic acid was investigated first, by incubating known amounts of humic acid and humic acid-coated nanospheres with an excess of BaP. A stock solution of humic acid was prepared by adding 10.1 mg of dried, purified humic acid (section 2.2) to 200 mL of deionized water, stirring for 2 hours, and filtering the resultant solution through a 0.45 μm HAWP Millipore filter under vacuum; this is designated the 50 mg/L humic acid solution. The 50 mg/L humic acid solution was then diluted into deionized water to make 0.01, 0.1, 0.5, and 1 mg/L humic acid solutions. Deionized water (no humic acid) served as a blank for the measurements. These solutions were analyzed by fluorimeter to determine if there is any interference from humic acid for the detection of BaP. Then, approximately 5 mg of solid BaP were added to those humic acid solutions, where BaP was placed in excess, and the vials were allowed to sit for one week in a dark environment. During the one week equilibration time, aliquots were periodically drawn from the vials and examined by fluorimeter for the analysis of any BaP that had been dissolved or adsorbed onto humic acid.

2.7 Preparation and Analysis of Benzo[a]pyrene on Humic acid-coated Particles

Similar to the procedure described in section 2.3, the first step in producing humic acid-coated nanospheres was to add twenty mL of SiO_2 stock solution to 4 mL of PLL

stock solution. As mentioned earlier, the SiO_2 stock solution has a particle concentration of 1.3066 mg/mL, and this 24 mL solution would therefore contain 26.1 mg of nanospheres. Since the added PLL serves only as an intermediary in adsorption of humic acid to the particles, the contribution of PLL was considered to be negligible in comparison to that of the silica nanospheres, and was not factored into calculation of the particle concentration. These PLL-coated SiO_2 nanospheres were then centrifuged at 10,000 rpm for 30 minutes, and the supernatant discarded. The particles were re-suspended in 10 mL of deionized water, and then combined with 30 mL of humic acid solution (section 2.3), resulting in a solution containing 653 mg/L of humic acid-coated nanospheres. This humic acid-coated particle solution is used in all the following experiments described in this section.

The 653 mg/L humic acid-coated particle solution was further diluted with deionized water to make a 20 mg/L particle solution, which was then used to prepare solutions with 0.01, 0.1, 0.5, and 1 mg/L of particles. Deionized water (no nanospheres) was also used as a control. After analyzing these solutions by fluorimeter to provide a baseline, approximately 5 mg of solid BaP was added to each vial, and the vials were allowed to sit for one week in a dark environment. During the 1 week equilibration time, an aliquot was withdrawn once every day from each vial for the BaP analysis by fluorimeter, using the BaP-only standards (Section 2.5).

2.8 Preparation and Analysis of Benzo[a]pyrene Incorporated into SUVs

The final step in the experiment examines the ability of SUVs to remove BaP that had been adsorbed onto humic acid-coated particles, and incorporate that BaP into the

liposome structure. A stock of BaP-saturated particles was made by adding approximately 10 mg of solid BaP to a 20 mg/L solution of humic acid-coated nanospheres, and allowing this to sit for one week in a dark environment. An aliquot was withdrawn from the bottom of the vial while avoiding the removal of any solid excess BaP during sampling. The aliquot was further diluted to 1 mg/L with deionized water and analyzed by fluorimeter to measure the concentration of BaP incorporated into the humic acid-coated particles.

Then, this BaP-incubated, 20 mg/L humic acid-coated particle solution was diluted to make a particle concentration of 1.0 mg/L in each vial, and then SUV stock solutions were added to make three different concentrations of 1000, 100, and 50 mg/L of vesicles. For this, a stock solution of 5 mg/mL SUVs was used to prepare the vials for the first condition, and one of 1 mg/mL SUVs was used to prepare the second and third conditions. Three replicates were made for each treatment tested in the present study. After all additions had been made, all prepared vials were allowed to sit in a dark environment for one week, with aliquots withdrawn each day for analysis.

Specifically, each day, 1 mL was withdrawn by pipette from each vial and centrifuged at 11,000 rpm for 30 minutes, to separate the humic acid-coated nanospheres from SUVs, which remained in suspension. This supernatant was diluted to produce two solutions with three replicates for each: a 1-to-10 dilution produced a 100 mg/L solution of SUVs, and a 1-to-20 dilution produced a 50 mg/L solution. The resulting six diluted solutions were analyzed by fluorimeter, and BaP concentrations were estimated using SUV Standard Set 1 for solutions containing 50 mg/L SUVs, and SUV Standard Set 2 for solutions containing 100 mg/L SUVs (Standard Sets from section 2.5). Only 5 days of

data are available for this part of the experiment. In parallel, the rest of the supernatant solutions were analyzed by fluorimeter without dilution for comparison.

CHAPTER THREE

RESULTS AND DISCUSSION

3.1 Synthesis and Characterization of Humic Acid-Coated Nanoparticles

3.1.1 Size and Zeta Potential Measurements

The z-average (Z_{ave}) hydrodynamic diameter and the surface charge of SiO_2 nanoparticles were measured to be 120.6 (± 1.1) nm and -63.3 (± 1.2) mV, at room temperature in an average pH of 7.85 (± 0.66). Any changes from these values, upon mixing with other solutions, were therefore attributed to alterations to the particle surfaces made by surrounding solution conditions. For instance, the SiO_2 stock solutions (section 2.3) were found to have a Z_{ave} hydrodynamic diameter of 113.8 (± 1.2) nm and a zeta potential of -13.6 (± 0.8) mV, in an average pH of 5.48 (± 0.01). The differences noted in the measured size and zeta potential values for the original SiO_2 particle solutions may be attributed to the presence of HEPES and NaCl in the Stock Solutions. A decrease in measured pH may be due to lowering the concentration of SiO_2 particles through dilution. The change in pH affected zeta potential values significantly, while affecting the particle size to a much lesser extent. Specifically, the initial zeta potential obtained from SiO_2 nanospheres alone reflects the negative surface charge developed through deprotonation of the hydroxyl groups by high solution pH. As pH decreases, protonation of the hydroxyl groups occurs, making the surface charge neutral or more positive.

Size and zeta potential measurements were made for a series of mixtures with the SiO_2 and PLL Stock Solutions listed in Table 2.1. With the addition of PLL having a positive overall charge, PLL-coated particles develop a net positive zeta potential in solution. The ability of PLL to adsorb to several types of surfaces has been previously established: PLL may adsorb to metal surfaces, such as gold, and form monolayers on carbon nanotubes without further chemical modification (Frey et al., 1995; Ling et al., 2014). PLL has also been used to bind proteins to surfaces through adsorption (Frey et al., 1995). In the same manner, PLL serves as an intermediary layer in this experiment, binding humic acid onto SiO_2 particles.

Figure 3.1 illustrates the trends in particle size and zeta potential as measured by DLS for the addition of PLL to silica nanospheres; the full data set may be found in Appendix A, as Table A.1. Since PLL provides positive surface charge on SiO_2 particles, the net surface charge decreased as the concentration of PLL in solution decreased, up to the 60:1 ratio, and then started to increase at 70:1, becoming more positive again. Similarly, particle size remained steady at approximately 130 – 140 nm up to the ratio of 50:1, and then with higher ratios of SiO_2:PLL, significant particle aggregation becomes evident. Further, precipitation of large particulates was also visually confirmed with ratios between 70:1 and 100:1. Particle aggregation and precipitation seems to occur when there is not enough PLL present to fully coat the SiO_2 particles. When the particles are partially coated with PLL, positively charged PLL bridges negatively charged SiO_2 nanoparticles, inducing significant particle aggregation. In this experiment, inclusion of further solutions at higher SiO_2:PLL ratios would likely have demonstrated decreasing

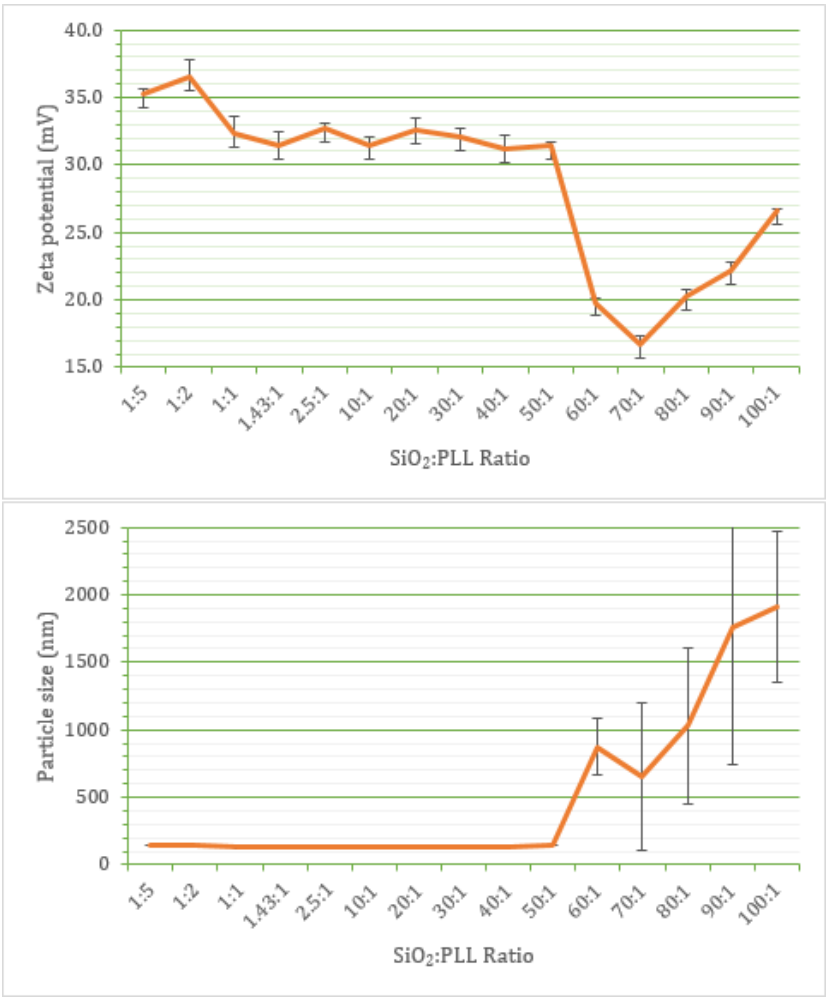

Figure 3.1. Measured zeta potential (top) and particle size (bottom) as a function of the relative concentrations of SiO_2 and PLL. Error bars represent one standard deviation (represented but not visible in size figure, ratios up to 50:1).

particle size and decreasing zeta potential as the amount of PLL present approached zero. This would be the result of fewer and fewer PLL bridges, so that less aggregation would occur, and of a lack of positively charged PLL in solution to counter the negative charge on SiO_2.

Based on the size and zeta potential data, we concluded that the 50:1 ratio solution had the minimum amount of PLL needed to cover the surface of the SiO_2

nanospheres, as the suspended particles become quickly unstable at higher ratios due to aggregation of particles only partially covered with PLL. Thus, the 50:1 ratio solution was used exclusively in further preparations with purified humic acid, using varying ratios specified in Table 2.2.

We found that the purified humic acid solution alone has a zeta potential of -42.1 mV in a solution pH of 5.61. Jovanović et al. (2013) found humic substances to have ca. -25 mV at pH 5.5. The difference in zeta potential values may be due to the type of source material and/or the difference of method used for the humic acid purification, as Jovanović et al. (2013) used the sieved powder prior to purification.

The addition of humic acid solution to the 50:1 SiO_2-PLL ratio was expected to produce a negative zeta potential in solution, due to the overall negative charge on the humic material, and an increase in observed particle size (relative to PLL coating only) upon successful sorption. Figure 3.2 illustrates trends in zeta potential and particle size for addition of humic acid; the full data set may be found in Appendix A, as Table A.2. Note that the ratios for these solutions are volume ratios, so that the 1:6 solution, for example, contains one milliliter of SiO_2-PLL particle solution and six milliliters of humic acid solution. When the zeta potential is positive, there is not enough humic acid present to counteract the charge from PLL. When the zeta potential is near zero, as near the 1:1 ratio solution, there would be very little free charge on any of the particles, inducing large particle aggregations; this is reflected in the sharp increase in particle size near 1:1. When surface charges increase, repulsion between particles also increases, forming smaller aggregates.

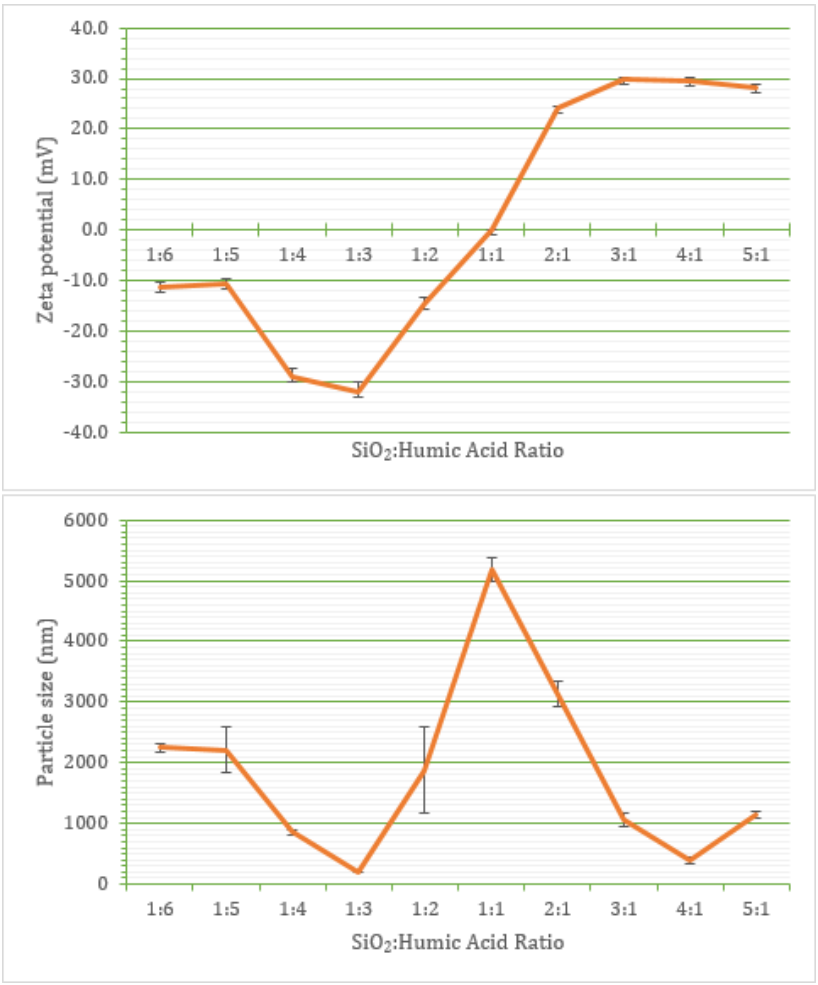

Figure 3.2. Measured zeta potential (top) and particle size (bottom) as a function of the volume ratio of PLL-coated SiO_2 solution to humic acid solution. Error bars represent one standard deviation.

The zeta potential became more negative with increasing humic acid concentration, and the lowest zeta potential value was found at the 1:3 ratio solution (-32.0 ± 2.1 mV). Further, the 1:3 ratio also recorded the smallest particle size (208.0 ± 1.0 nm), indicating that negative surface charge posed by the humic acid coating on the particle surface induces particle dispersion while preventing aggregation. Therefore this ratio was chosen for the later batch experiments with BaP and SUVs.

3.1.2 Thermogravimetric Analysis

Thermogravimetric analysis (TGA) is a method that monitors the mass of a sample over time as the temperature changes. TGA can therefore provide information about physical phenomena of the sample such as phase transitions, absorption and desorption, and thermal decomposition. For example, this method has been used to determine water loss kinetics in polyvinyl chloride (PVC) beads; this is important in PVC production as the powder must be stored dry (Agaciak et al., 2015). TGA may be used in conjunction with another method such as mass spectrometry, for example, to study the thermal desorption of oleylamine from platinum nanoparticles (Humphrey et al., 2015).

In this study, thermogravimetric analysis (TGA) was therefore used to confirm the successful sorption of PLL and/or humic acid on the SiO_2 nanoparticles. Results of TGA are summarized in Figure 3.3. The solutions with SiO_2:humic acid ratios between 1:2 and 1:6 were chosen for TGA because zeta potential values for these solutions were negative, indicating the presence of humic acid on the surface, which should produce a notable signature in TGA data. A 50:1 SiO_2:PLL particle solution without humic acid was also analyzed, and showed a slight flattening at 97% weight.

The weight loss between 25°C and 200°C can be attributed to the removal of water from the samples. If the samples had been held isothermally at ~ 100-150°C until there was no further weight loss, there would have been a longer, flatter plateau region. Except for the 1:5 composition, the loss of water is ~ 2.5% for all samples. Note that the "increase" in apparent weight at 800°C for all the samples is an artifact that arises due to static repulsion of the samples when they are very dry.

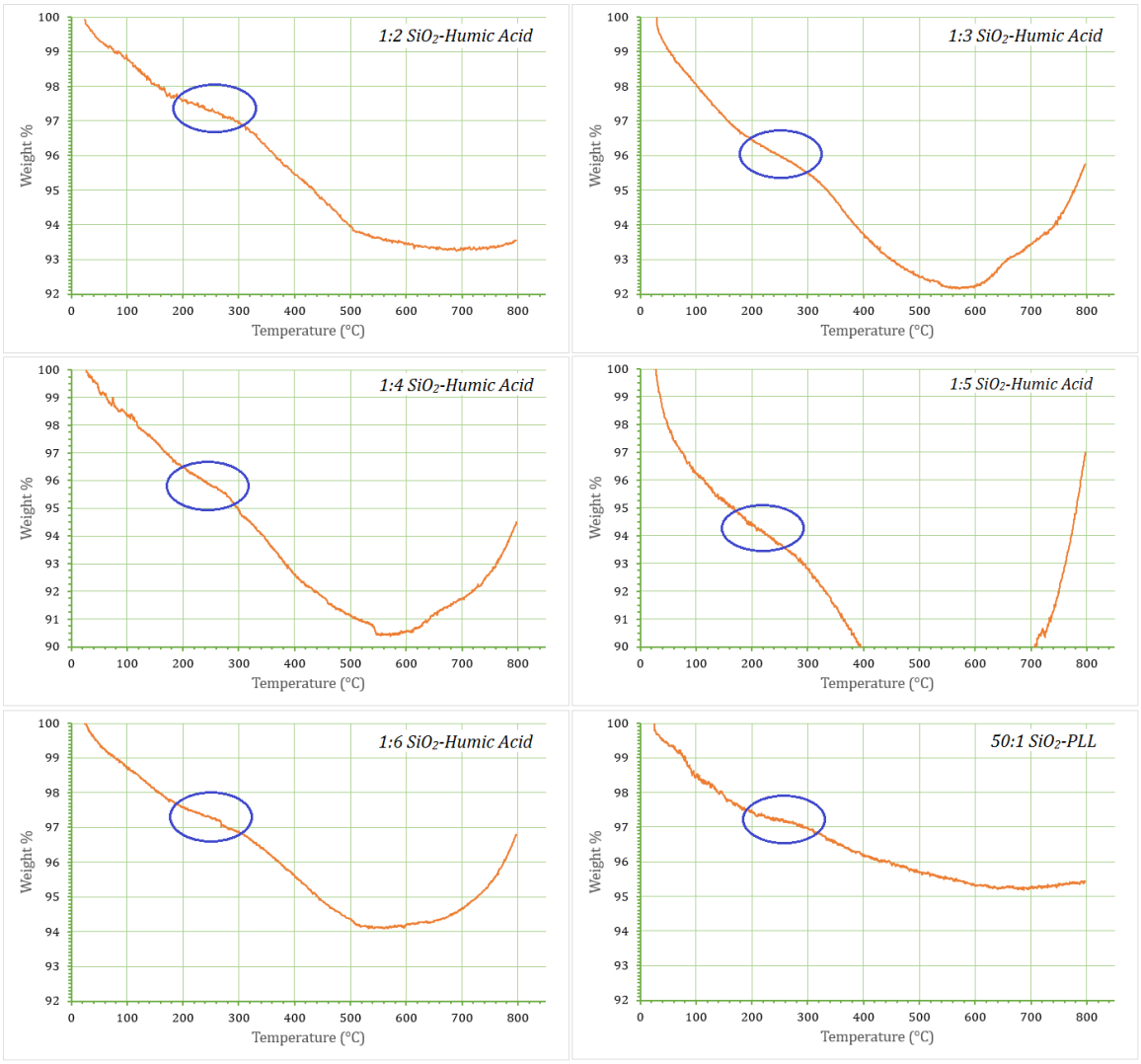

Figure 3.3. Results of thermogravimetric analysis for SiO_2-humic acid particles, ratios ranging from 1:2 through 1:6. The analysis of 50:1 SiO_2-PLL serves as a control with no humic acid. Plateaus noted within circled regions.

For the SiO_2 sample with only adsorbed PLL, the total weight loss is ~ 4.5%, so that the amount attributed to PLL is ~ 2%. As the SiO_2-PLL/humic acid ratio decreases (i.e., more humic acid is added), the weight loss also increases. After subtracting the weight loss due to H_2O and PLL (6.5%), the weight loss due to the humic acid is 2% for

1:2, 2.5% for 1:3, 4% for 1:4, and 6% for 1:5. The sample at 1:6 has only a 1.5% weight loss for humic acid and is anomalous.

3.2 Optimization of Parameters for Fluorimeter Analysis

For fluorimeter analysis, it was necessary to choose the wavelengths of excitation and emission at which BaP produced the strongest signal that was free from other interferences. Therefore, a solution of BaP (0.008 μM) and three solutions of humic acid (1, 5, and 10 mg/L) were analyzed in multiple excitation and emission scans. BaP consistently produces its strongest emission at 405 nm.

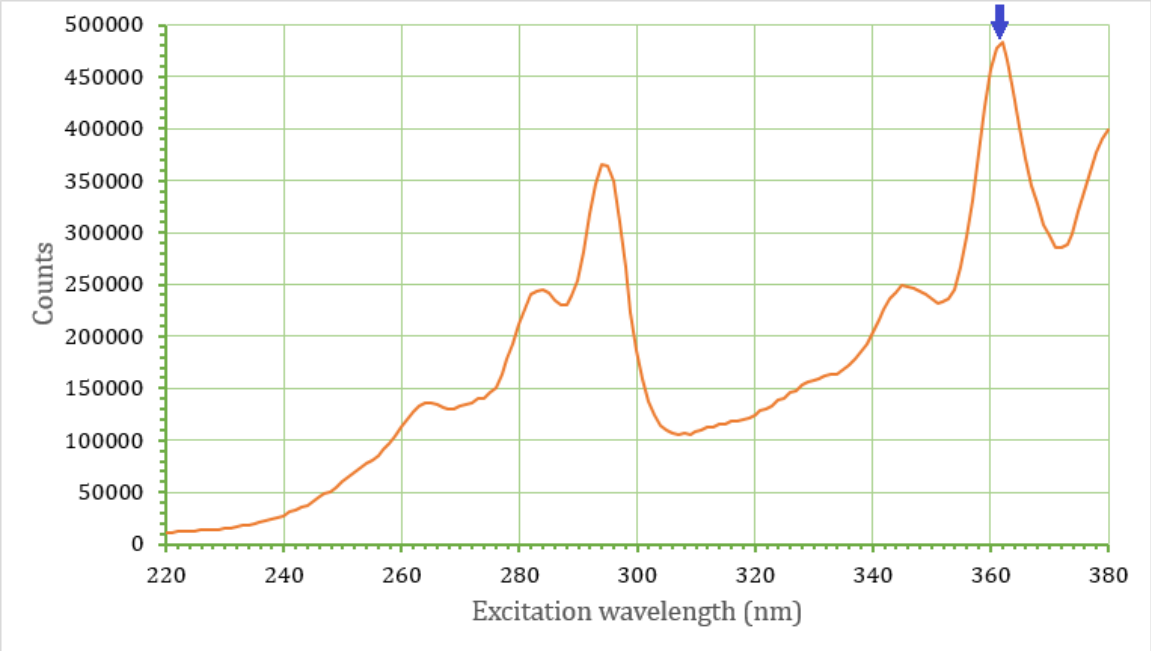

Figure 3.4. An excitation fluorescence spectrum of 0.008 μM benzo[a]pyrene in acetonitrile, from 220 nm to 380 nm, reading emission at 405 nm. The strongest excitation wavelength was observed at 362 nm (marked by arrow).

As seen in Figure 3.4, the strongest response from BaP was found at an excitation wavelength of 362 nm. To identify possible interferences originating from humic acid at the excitation wavelength (362 nm), a solution of 1 mg/L humic acid was analyzed under the same conditions; the results are presented as figure 3.5.

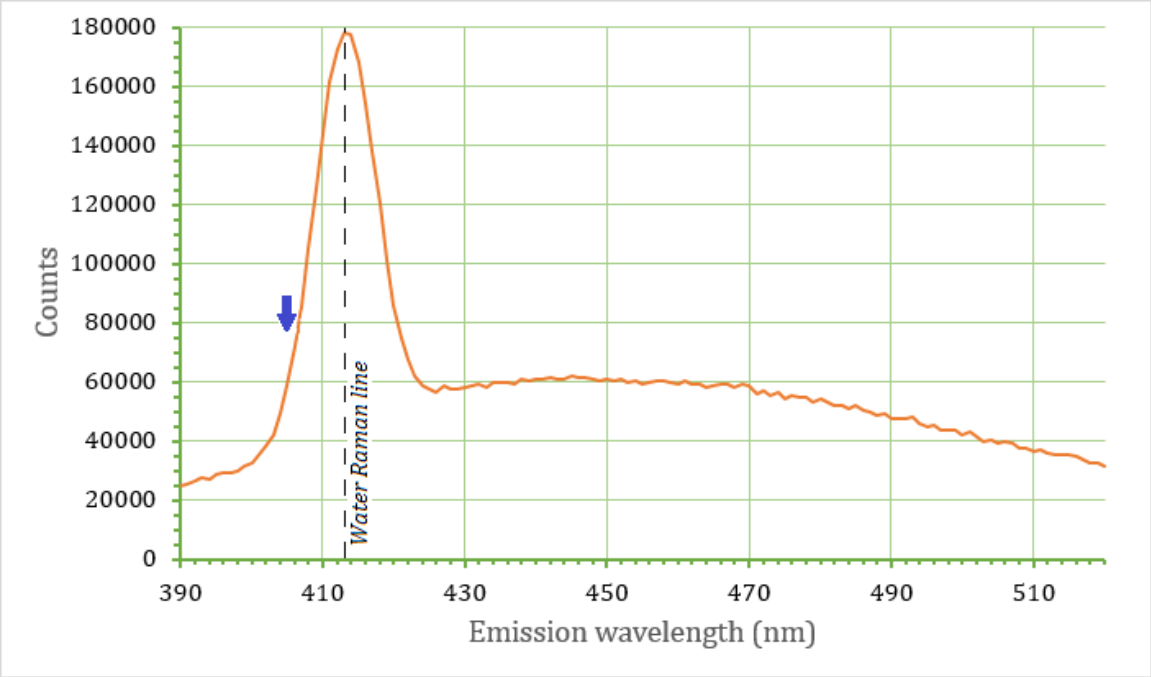

Figure 3.5. An emission fluorescence spectrum of 1 mg/L humic acid in water, from 390 nm to 520 nm, using an excitation wavelength of 362 nm. The peak at 413 nm is the Raman line for water. The arrow marks emission at 405 nm, used in further experiments.

As shown in Figure 3.5, the humic acid response is low in counts over the entire scan range in comparison to Figure 3.4. For instance, the measured counts of humic acid for emission at 405 nm are 58,770, whereas the response from BaP is over 450,000 (approximately 8 times higher), indicating an insignificant interference. The Raman shift peak for water is found at 413 nm.

3.3 Fluorimeter Analysis of Humic Acid and Benzo[a]pyrene in Solution

By testing concentrations of 0.01, 0.1, 0.5, and 1.0 mg/L of humic acid only, it is apparent that increasing humic acid concentration results in a stronger fluorescent signal (Figure 3.6); the increase is on the order of 5000 counts or less between each analysis and can be considered minimal, especially at 405 nm, where the strongest emission of BaP is found. Thus, the background subtraction of humic acid is not performed in later experiments with BaP.

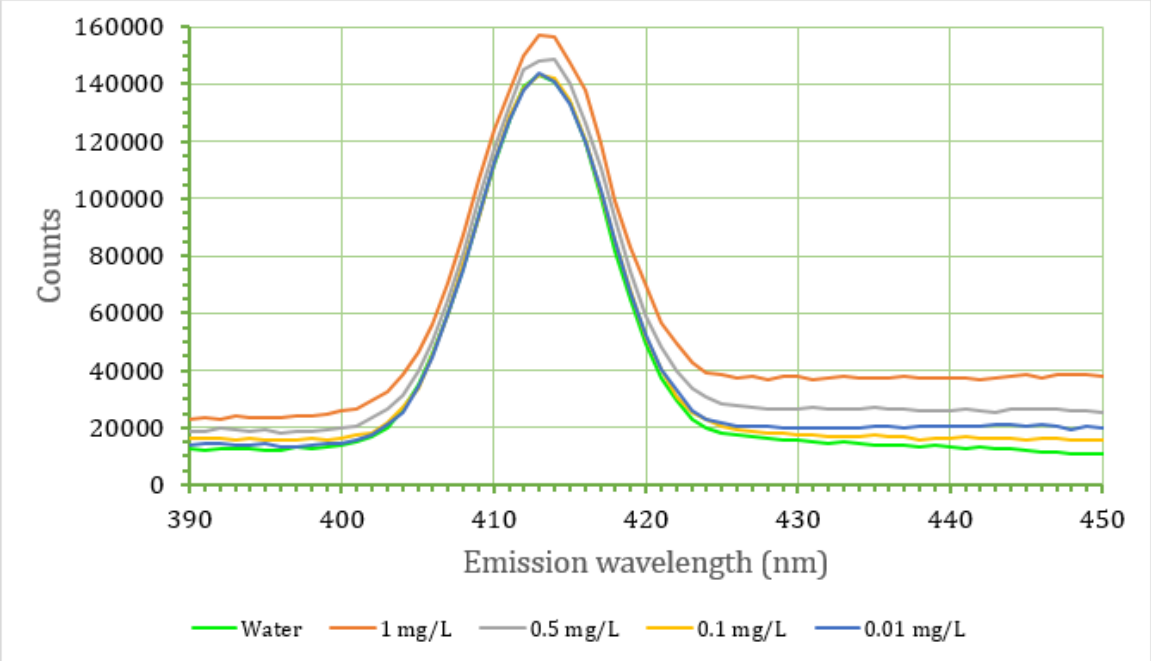

Figure 3.6. Fluorescence spectra of humic acid solutions at several concentrations, along with deionized water for comparison. Excitation at 362 nm.

Solid benzo[a]pyrene was added to the aforementioned humic acid solutions (0.01, 0.1, 0.5, and 1.0 mg/L**)** and then analyzed by fluorimeter at 36 hours, 60 hours, and one week after addition, to monitor any changes in the fluorescence responses with

increasing equilibration time. Figure 3.7 presents the resulting spectra, and each spectrum includes a scan of deionized water for reference (the Raman shift peak for water at 413 nm). Each spectrum includes the two peaks characteristic of the fluorescence of BaP, one at 405 nm and one at 428 nm. At 405 nm, all solutions displayed an approximately 3.5-fold increase in signal with addition of BaP after one week, indicating the amount of BaP extracted by humic acid increased over time (although it was not quantified). With the exception of the solution containing 0.1 mg/L humic acid and BaP, the signal for each solution remained the same between 60 hours and one week, indicating that equilibrium had been reached by 60 hours and thus, no more additional BaP incorporated by humic acid. The unusually high response measured in the solution containing 0.1 mg/L humic acid may be attributed to experimental errors that may have occurred in sample handling and withdrawal for the fluorescence measurements. For instance, it is possible that very fine-scale BaP particles may have been taken unintentionally into the aliquots for the analysis. This may also explain the high fluorescence response obtained from the 0.01 mg/L humic acid solution when measured at 60 hours. The non-linear increase in peak heights was observed for all solutions as particle concentrations increased.

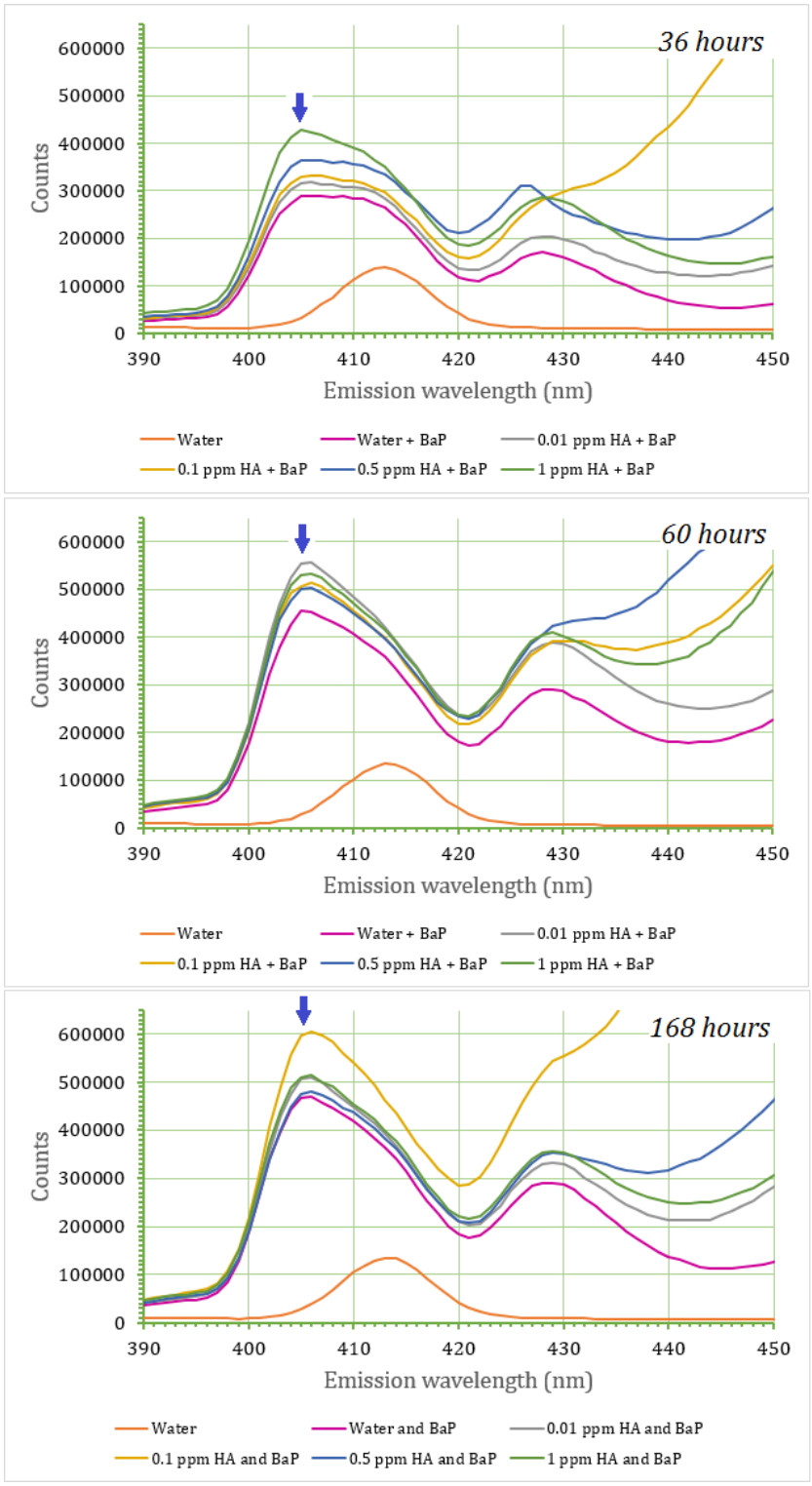

Figure 3.7. Fluorescence spectra of humic acid solutions from 0.01 to 1.0 mg/L, after addition of BaP, at 36 hours (top), 60 hours (middle), and one week (bottom) after addition. Excitation at 362 nm. Arrows mark emission at 405 nm, used in further testing.

3.4 Quantification of Benzo[a]pyrene with Humic Acid-Coated SiO_2 Nanospheres

The same experimental procedure performed in Section 3.3 was repeated with humic acid-coated nanospheres, and BaP was quantified in these tests (Section 2.7). Estimated BaP concentrations (micrograms of BaP per liter) are shown in Figure 3.8 and summarized in Table A.5 (Appendix A), organized by concentrations of humic acid-coated SiO_2 nanospheres. Calibration curves and raw data for BaP quantification may also be found in Appendix A, as Tables A.3 and A.4.

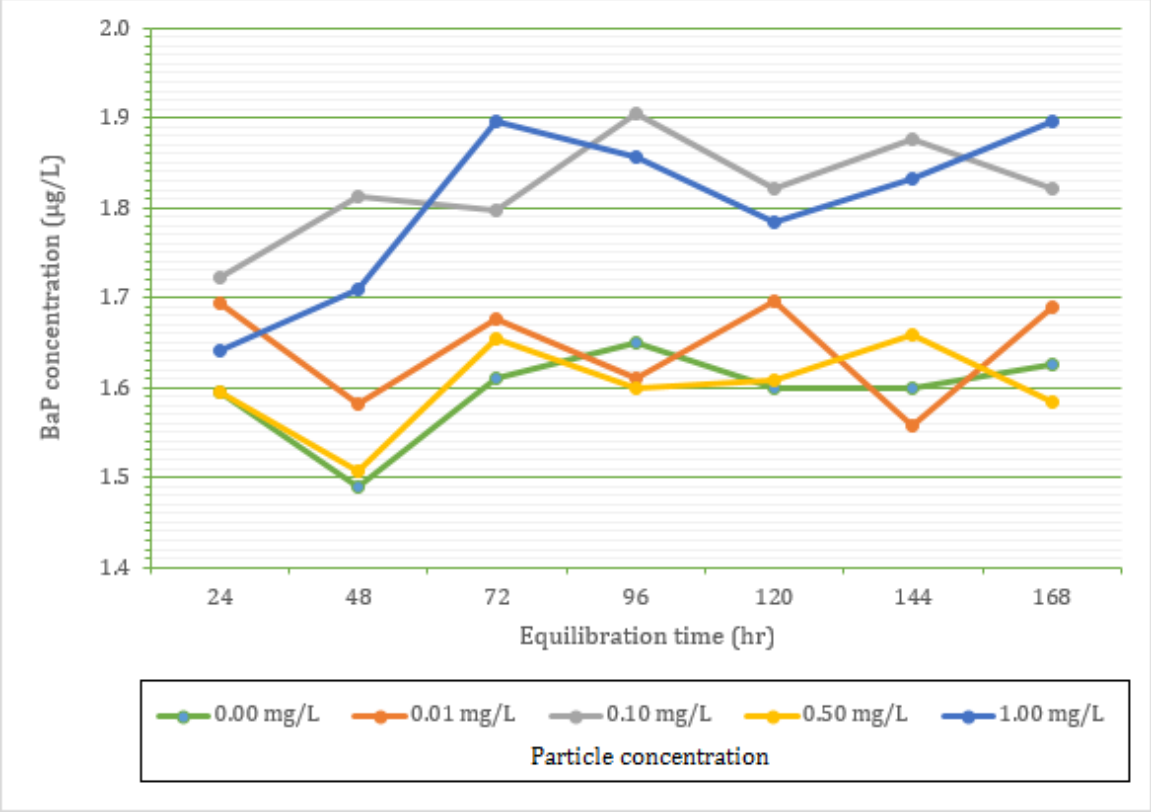

Figure 3.8. BaP concentration extracted by humic acid-coated SiO_2 nanospheres over time, tested with several particle concentrations. Standard deviation could not be calculated for this data, as only one preparation was made for each particle concentration.

As shown in Figure 3.8, an increase in BaP is generally accompanied with both increased equilibration time and an increase in particle concentration: the highest result was found to be 1.90 μg/L, at 168 hours, in the solution containing 1.00 mg/L of particles. By comparison, the concentration of BaP in the water blank at 168 hours was found to be 1.63 μg/L. However, exceptions were found with the solutions containing 0.10 mg/L and 0.50 mg/L of particles, which did not present concentration-dependent responses. It is possible that a dilution error occurred upon initial preparation, resulting in the incorrect amount of particles, or that vials were accidentally mis-labeled.

In parallel, a solution was prepared containing 20 mg/L of humic acid-coated particles, and allowed to saturate with BaP over one week (Section 2.6). Out of the 1 mg/L solutions prepared from this stock, three were randomly chosen and analyzed by fluorimeter to determine the concentration of BaP available for SUVs to incorporate in the following experiment. The average result was found to be 1.77 ± 0.036 μg/L of BaP, marginally lower than (but comparable to) the BaP concentrations found in the solutions containing 1.0 mg/L of nanospheres without dilution; this was 1.90 μg/L after one week. The 1.0 mg/L solutions of particles prepared from the BaP-saturated stock were used in the following experiment.

Finally, SUVs were introduced to incorporate BaP from BaP-saturated humic acid-SiO_2 nanoparticles in triplicate. Calibration curves, raw data, and final results may be found in Appendix A, as Tables A.6 through A.10.

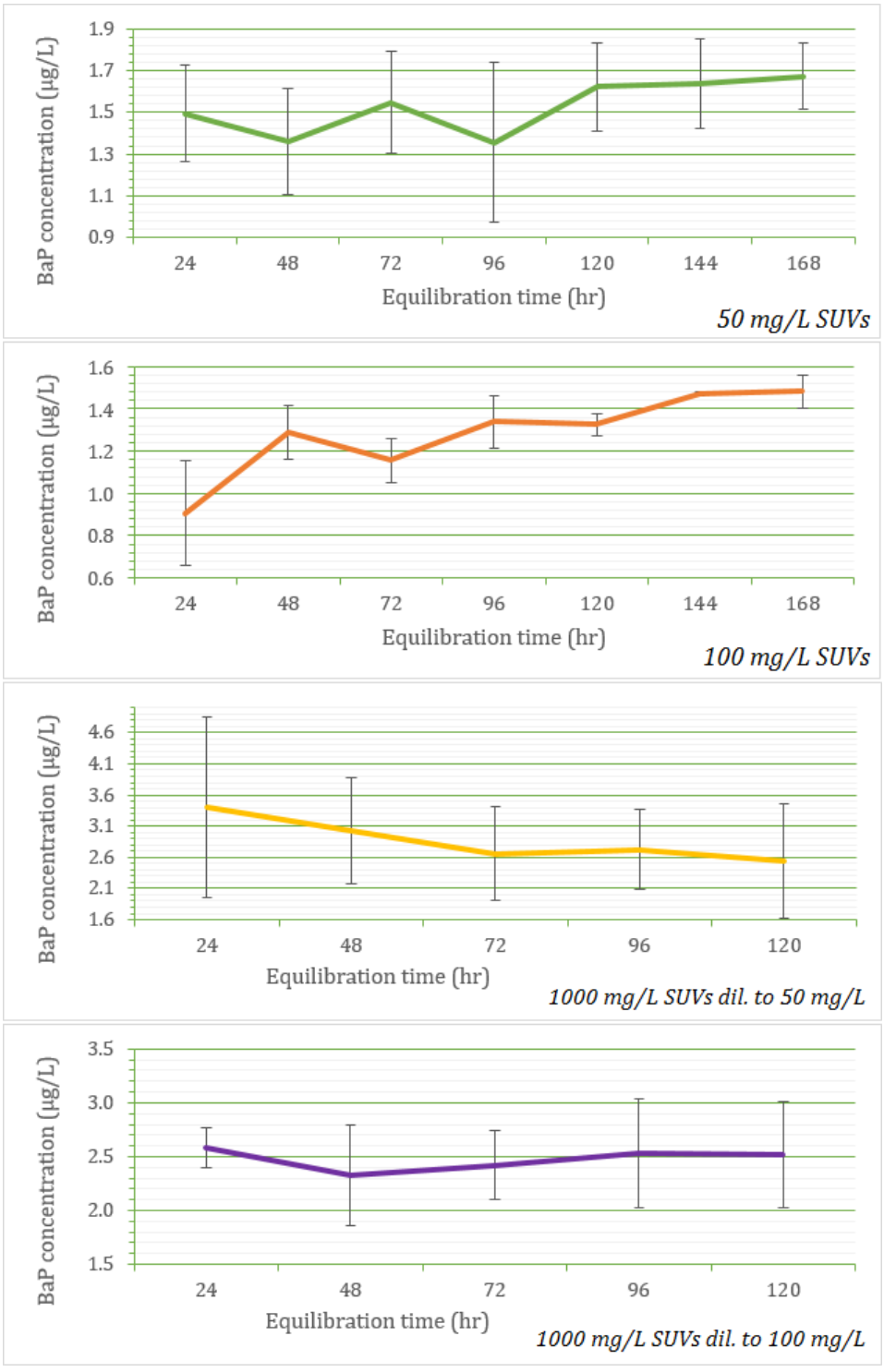

Figure 3.9. Quantity of BaP taken up by SUVs after equilibration times up to one week. Solutions containing 50 mg/L SUVs (top), 100 mg/L SUVs (second from top), 1000 mg/L SUVs diluted to 50 mg/L for analysis (second from bottom), and 1000 mg/L SUVs diluted to 100 mg/L for analysis (bottom). Error bars represent one standard deviation.

As illustrated in Figure 3.9, in general, there is a slight increase in BaP concentration with increased equilibration time, and the solutions containing 50 mg/L of SUVs incorporate the most BaP over a week's equilibration time amongst the tested SUVs concentrations. Since the vials were allowed to equilibrate at room temperature, it is possible that the liposomes in some vials lost their structural integrity more quickly than in others, or began to degrade. This may be also responsible for a larger standard deviation noted after one week. Wang et al. (2015) did not observe any change in SUV particle size after a two week period, either alone or in the presence of BaP; however, humic acid in their solutions was suspended, as opposed to anchored (in this work). At the end of the week, the results of mass balance calculations for the 50 mg/L (BaP 1.67 μg/L) and 100 mg/L (BaP 1.48 μg/L) SUV solutions indicated that not all BaP adsorbed to the humic acid-coated particles was removed by the SUVs. However, the results for the two dilutions of 1000 mg/L SUV solution are higher than these initial values (2.55 and 2.52 μg/L). Such error may arise from the presence of very fine-scale, solid BaP particles, which were unintentionally added to the testing vials when they were diluted from the stock of BaP-saturated 20 mg/L humic acid-SiO_2 particles.

The recovery of BaP by SUVs may be calculated using the known BaP concentration on 1 mg/L solutions of BaP-saturated nanospheres. These were analyzed before addition of SUVs and their average BaP concentration was 1.77 μg/L. The solution with 50 mg/L of SUVs therefore showed a 94.6% recovery of BaP present on humic acid-SiO_2 nanospheres, and the solution with 100 mg/L of SUVs showed an 83.8% recovery. A comparable study in the literature, performed by Luo et al. (2007), achieved 93.3% to 100.1% recovery of BaP from humic acid bonded covalently to silica. The

method followed by Luo et al. (2007) did not utilize SUVs, but employed fluorescence analysis for quantification, and humic acid served as the reagent to remove BaP from a set of edible oils. To my knowledge, this thesis work provides for the first time the evidence that lipid vesicles can effectively solubilize BaP that was originally bound onto humic acids.

3.5 Conclusions

The purpose of this thesis was to assess the suitability of SUVs for potential use in PAH remediation in the environment. Specifically, whether SUVs could help enhance the solubility of PAHs that were originally bound onto soil organic matter or not was of special interest. First, the synthesis of a composite nanoparticle containing PLL and humic acid was performed to serve as an analog of natural humic acid coated-mineral oxides in the environment. This composite requires less preparation time with simplified experimental procedures, offering an advantage over traditional SiO_2-humic acid systems, where grafting of humic acid through multiple steps requires time-consuming curing and stirring (Koopal et al., 1998). It is noted, however, that the physical stability of the composite system appears to be affected by changes such as centrifugation and solution pH. Therefore, future work is needed to optimize experimental parameters to improve its stability for its wider use as an organic-mineral environmental surrogate in batch reactions.

DLS results for size and zeta potential demonstrate that a monolayer of PLL may be adsorbed to the surface of a SiO_2 nanosphere, around a concentration ratio of 50:1 SiO_2:PLL. A layer of humic acid may then be adsorbed, using a volume ratio of 1:3 PLL-

SiO_2 (v:v) particle solution to humic acid solution; the final product was found to have a hydrodynamic diameter of 208 nm and a zeta potential at -32.0 mV. Based on particle size and zeta potential measurements, therefore, the first hypothesis (Section 1.5) is confirmed in that PLL serves adequately as an intermediate reagent to add humic acid onto SiO_2 nanospheres in the solution.

Secondly, the solubility of BaP was monitored in the presence of these humic acid-coated SiO_2 particles. An increase in BaP is then a result of solid BaP migrating onto humic acid-SiO_2 particles that were suspended in the solution. A solution containing 1 mg/L of these particles was found to contain BaP at a concentration of 1.90 μg/L after equilibrating for one week.

Finally, SUVs were introduced to BaP-humic acid-SiO_2 particles and incubated for one week at room temperature to see whether BaP can effectively migrate into SUVs from humic acid-SiO_2 particles. In the presence of SUV concentrations of 50 mg/L and 100 mg/L, 94.4% and 83.6% (respectively) of the added BaP was found to be incorporated into SUVs from humic acid-SiO_2 particles. In the presence of 1,000 mg/L SUVs, the recovery was found to be anomalously high (greater than 100%), but this is likely an effect of the dilutions necessary for quantitation. Therefore, the second hypothesis (Section 1.5) is also confirmed in that SUVs can effectively incorporate BaP which had been adsorbed onto humic acid in the structure, and that this can be measured through fluorescence. However, the methods presented in this thesis may require future work for optimization. For example, a method may be devised for effective removal of fine BaP solids from solutions after the humic acid-coated particles are fully saturated.

These results indicate SUVs being a potentially useful tool for use in remediation of soil and sediment, as it has been demonstrated that BaP may be desorbed from humic acid in preference for the hydrophobic interior of the vesicles' bilayer. This can increase their accessibility to a group of soil microorganisms which can effectively degrade persistent PAHs in the environment (Wang et al., 2015). However, for a field-scale trial, it is still necessary to assess the suitability and stability of SUVs in the actual environment, where mineral mixtures and impurities and co-presence of contaminants that can affect microbial populations and activities exist. Thus, continuing effort needs to be made to optimize experimental conditions for SUVs as another possible tool for PAH remediation.

REFERENCES CITED

Agaciak, P., Yahiaoui, S., Djabourov, M., and Lasuye, T., 2015, Dehydration and drying poly(vinyl)chloride (PVC) porous grains: 2. Thermogravimetric analysis and numerical simulations: Colloids and Surfaces A: Physicochemical and Engineering Aspects, v. 470, p. 120-129, doi:10.1016/j.colsurfa.2015.01.020.

Ayyildiz, H.F., 2015, Evaluation of new silica-based humic acid stationary phase for the separation of tocopherols in cold-pressed oils by normal-phase high-performance liquid chromatography: Journal of Separation Science, v. 38, p. 813-820, doi:10.1002/jssc.201401377.

Chen, K., and Elimelech, M., 2008, Interaction of Fullerene (C_{60}) Nanoparticles with Humic Acid and Alginate Coated Silica Surfaces: Measurements, Mechanisms, and Environmental Implications: Environmental Science & Technology, v. 42, p. 7607-7614, doi:10.1021/es8012062.

Comprehensive Environmental Response, Compensation, and Liability Act, 42 U.S.C. §§ 9601-9675 (2012).

Crane, R.A., and Scott, T.B., 2012, Nanoscale zero-valent iron: Future prospects for an emerging water treatment technology: Journal of Hazardous Materials, v. 211-212, p. 112-125, doi:10.1016/j.jhazmat.2011.11.073.

De Maagd, P.G., Ten Hulscher, D., Van Den Heuvel, H., Opperhuizen, A., and Sijm, D., 1998, Physicochemical properties of polycyclic aromatic hydrocarbons: Aqueous solubilities, n-octanol/water partition coefficients, and Henry's law constants: Environmental Toxicology and Chemistry, v. 17, p. 251-257, doi:10.1002/etc.5620170216.

Ferrarese, E., Andreottola, G., and Oprea, I.A., 2008, Remediation of PAH-contaminated sediments by chemical oxidation: Journal of Hazardous Materials, v. 152, p. 128-139, doi:10.1016/j.jhazmat.2007.06.080.

Frey, B.L., Jordan, C.E., Kornguth, S., and Corn, R.M., 1995, Control of the specific adsorption of proteins onto gold surfaces with poly(L-lysine) monolayers: Analytical Chemistry, v. 67, p. 4452-4457, doi:10.1021/ac00120a003.

Garcia-Flores, E., Wakida, F.T., Rodríguez-Mendivil, D.D., and Espinoza-Gomez, H., 2016, Polycyclic Aromatic Hydrocarbons in Road-Deposited Sediments and Roadside Soil in Tijuana, Mexico: Soil and Sediment Contamination: An International Journal, v. 25, p. 223-239, doi:10.1080/15320383.2016.1113497.

Gómez, J., Alcántara, M.T., Pazos, M., and Sanromán, M.A., 2009, A two-stage process using electrokinetic remediation and electrochemical degradation for treating benzo[a]pyrene spiked kaolin: Chemosphere, v. 74, p. 1516-1521, doi:10.1016/j.chemosphere.2008.11.019.

Gramss, G., Voigt, K., and Kirsche, B., 1999, Oxidoreductase enzymes liberated by plant roots and their effects on soil humic material: Chemosphere, v. 38, p. 1481-1494, doi:10.1016/S0045-6535(98)00369-5.

Haigh, S.D., 1996, A review of the interaction of surfactants with organic contaminants in soil: Science of the Total Environment, v. 185, p. 161-170, doi:10.1016/0048-9697(95)05049-3.

Humphrey, J., Sadasivan, S., Plana, D., Celorrio, V., Tooze, R.A., and Fermín, D.J., 2015, Surface Activation of Pt Nanoparticles Synthesised by "Hot Injection" in the Presence of Oleylamine: Chemistry – A European Journal, v. 21, p. 12694-12701, doi:10.1002/chem.201501496.

Joo, J.C., Shackelford, C.D., and Reardon, K.F., 2008, Association of humic acid with metal (hydr)oxide-coated sands at solid-water interfaces: Journal of Colloid and Interface Science, v. 317, p. 424-433, doi:10.1016/j.jcis.2007.09.061.

Jovanović, U.D., Marković, M.M., Cupać, S.B., and Tomić, Z.P., 2013, Soil humic acid aggregation by dynamic light scattering and laser Doppler electrophoresis: Journal of Plant Nutrition and Soil Science, v. 176, p. 674-679, doi:10.1002/jpln.201200346.

Koopal, L.K., Yang, Y., Minnaard, A.J., Theunissen, P.L.M., and Van Riemsdijk, W.H., 1998, Chemical immobilisation of humic acid on silica: Colloids and Surfaces A: Physicochemical and Engineering Aspects, v. 141, p. 385-395, doi:10.1016/S0927-7757(97)00170-2.

Lamichhane, S., Bal Krishna, K.C., and Sarukkalige, R., 2017, Surfactant-enhanced remediation of polycyclic aromatic hydrocarbons: A review: Journal of Environmental Management, v. 199, p. 46-61, doi:10.1016/j.jenvman.2017.05.037.

Lin, J., Zhan, Y., and Zhu, Z., 2011, Adsorption characteristics of copper (II) ions from aqueous solution onto humic acid-immobilized surfactant-modified zeolite: Colloids and Surfaces A: Physicochemical and Engineering Aspects, v. 384, p. 9-16, doi:10.1016/j.colsurfa.2011.02.044.

Ling, X., Wei, Y., Zou, L., and Xu, S., 2014, Functionalization and dispersion of multiwalled carbon nanotubes modified with poly-l-lysine: Colloids and Surfaces A: Physicochemical and Engineering Aspects, v. 443, p. 19-26, doi:10.1016/j.colsurfa.2013.10.053.

Luo, D., Yu, Q., Yin, H., and Feng, Y., 2007, Humic acid-bonded silica as a novel sorbent for solid-phase extraction of benzo[a]pyrene in edible oils: Analytica Chimica Acta, v. 588, p. 261-267, doi:10.1016/j.aca.2007.02.016.

MacCarthy, P., 2001a, The Principles of Humic Substances: Soil Science, v. 166, p. 738-751, doi:10.1097/00010694-200111000-00003.

MacCarthy, P., 2001b, The principles of humic substances: An introduction to the First Principle, *in* Davies, G., and Ghabbour, E.A., eds., Humic Substances: Structures, Models and Functions: Royal Society of Chemistry, Cambridge, p. 17-28.

Machado, S., Stawiński, W., Slonina, P., Pinto, A.R., Grosso, J.P., Nouws, H.P.A., Albergaria, J.T., and Delerue-Matos, C., 2013, Application of green zero-valent iron nanoparticles to the remediation of soils contaminated with ibuprofen: Science of the Total Environment, v. 461-462, p. 323-329, doi:10.1016/j.scitotenv.2013.05.016.

Maire, J., Coyer, A., and Fatin-Rouge, N., 2015, Surfactant foam technology for in situ removal of heavy chlorinated compounds-DNAPLs: Journal of Hazardous Materials, v. 299, p. 630-638, doi:10.1016/j.jhazmat.2015.07.071.

Martin, R.J., 1998, EPA Ombudsman Final Report on the Drake Chemical Superfund Site: Remediation Journal, v. 8, p. 29-45, doi:10.1002/rem.3440080405.

Mosca Angelucci, D., and Tomei, M.C., 2015, Regeneration strategies of polymers employed in ex-situ remediation of contaminated soil: Bioregeneration versus solvent extraction: Journal of Environmental Management, v. 159, p. 169-177, doi:10.1016/j.jenvman.2015.05.018.

Mulligan, C.N., Yong, R.N., and Gibbs, B.F., 2001, Surfactant-enhanced remediation of contaminated soil: a review: Engineering Geology, v. 60, p. 371-380, doi:10.1016/S0013-7952(00)00117-4.

Nyer, E.K., 2001, In situ treatment technology: Boca Raton, Lewis Publishers, 552 p.

Pei, G., Zhu, Y., Cai, X., Shi, W., and Li, H., 2017, Surfactant flushing remediation of o-dichlorobenzene and p-dichlorobenzene contaminated soil: Chemosphere, v. 185, p. 1112-1121, doi:10.1016/j.chemosphere.2017.07.098.

Perelo, L.W., 2010, Review: In situ and bioremediation of organic pollutants in aquatic sediments: Journal of Hazardous Materials, v. 177, p. 81-89, doi:10.1016/j.jhazmat.2009.12.090.

Perminova, I., and Hatfield, K., 2005, Remediation Chemistry of Humic Substances: Theory and Implications for Technology, *in* Perminova, I.V., Hatfield, K., and Hertkorn, N., eds., Use of Humic Substances to Remediate Polluted

Environments: From Theory to Practice: Springer Netherlands, Dordrecht, p. 3-36, doi:10.1007/1-4020-3252-8_1.

Reddy, K.R., and Cameselle, C., 2009, Overview of Electrochemical Remediation Technologies, *in* Reddy, K.R., and Cameselle, C., eds., Electrochemical Remediation Technologies for Polluted Soils, Sediments and Groundwater: John Wiley & Sons, Inc., Hoboken, p. 1-28, doi:10.1002/9780470523650.

Shaw, D.G., Maczynski, A., Goral, M., and Wisniewska-Goclowska, B., 2006a, IUPAC-NIST Solubility Data Series. 81. Hydrocarbons with Water and Seawater—Revised and Updated. Part 9. C10 Hydrocarbons with Water: Journal of Physical and Chemical Reference Data, v. 35, p. 93-151, doi:10.1063/1.2131103.

Shaw, D.G., Maczynski, A., Goral, M., and Wisniewska-Goclowska, B., 2006b, IUPAC-NIST Solubility Data Series. 81. Hydrocarbons with Water and Seawater—Revised and Updated. Part 11. C13 – C36 Hydrocarbons with Water: Journal of Physical and Chemical Reference Data, v. 35, p. 687-784, doi:10.1063/1.2132315.

Siegrist, R.L., Crimi, M., and Brown, R.A., 2011, In Situ Chemical Oxidation: Technology Description and Status, *in* Siegrist, R.L., Crimi, M. and Simpkin, T.J., eds., In Situ Chemical Oxidation for Groundwater Remediation: Springer-Verlag, New York, p. 1-32, doi:10.1007/978-1-4419-7826-4_1.

Stevenson, F.J., 1994, Humus chemistry: genesis, composition, reactions: New York, John Wiley & Sons, 443 p.

Tang, W., Zeng, G., Gong, J., Liang, J., Xu, P., Zhang, C., and Huang, B., 2014, Impact of humic/fulvic acid on the removal of heavy metals from aqueous solutions using nanomaterials: A review: Science of the Total Environment, v. 468-469, p. 1014-1027, doi:10.1016/j.scitotenv.2013.09.044.

Tomei, M.C., Mosca Angelucci, D., Ademollo, N., and Daugulis, A.J., 2015, Rapid and effective decontamination of chlorophenol-contaminated soil by sorption into commercial polymers: Concept demonstration and process modeling: Journal of Environmental Management, v. 150, p. 81-91, doi:10.1016/j.jenvman.2014.11.014.

Tsai, T.T., Kao, C.M., and Wang, J.Y., 2011, Remediation of TCE-contaminated groundwater using acid/BOF slag enhanced chemical oxidation: Chemosphere, v. 83, p. 687-692, doi:10.1016/j.chemosphere.2011.02.023.

U.S. Environmental Protection Agency, 2018, Metal Bank Superfund Site Profile, U.S. EPA: https://cumulis.epa.gov/supercpad/cursites/csitinfo.cfm?id=0300951 (accessed 12/6 2018).

Walker, C.H., 2008, Organic Pollutants: An Ecotoxicological Perspective: Boca Raton, CRC Press/Taylor & Francis, 408 p.

Wang, H., Kim, B., and Wunder, S.L., 2015, Nanoparticle-supported lipid bilayers as an in situ remediation strategy for hydrophobic organic contaminants in soils: Environmental Science & Technology, v. 49, p. 529-536, doi:10.1021/es504832n.

Wuana, R.A., and Okieimen, F.E., 2011, Heavy Metals in Contaminated Soils: A Review of Sources, Chemistry, Risks and Best Available Strategies for Remediation: ISRN Ecology, v. 2011, 402647, doi:10.5402/2011/402647.

Zhang, W., and Elliott, D.W., 2006, Applications of iron nanoparticles for groundwater remediation: Remediation, v. 16, p. 7-21, doi:10.1002/rem.20078.

APPENDIX A

FULL DATA SETS OF EXPERIMENTAL RESULTS

Tables A.1 and A.2 are referenced in Section 3.1, and contain the data sets for preparation of PLL-coated and humic acid-coated SiO_2 nanospheres. Tables A.3 through A.10 correspond to Section 3.4.

Table A.1

Zeta Potential and Size Measurements for Varying SiO_2:PLL Ratios

Ratio	Zeta potential (mV)			Particle size (nm)			Average	
	Prep 1	Prep 2	Prep 3	Prep 1	Prep 2	Prep 3	Zeta (mV)	Size (nm)
1:5	34.9	35.3	35.6	144.0	143.2	144.2	35.3±0.35	143.8±0.5
1:2	36.0	38.0	35.7	141.3	139.9	141.5	36.6±1.25	140.9±0.9
1:1	33.5	31.1	32.5	125.1	128.3	126.2	32.4±1.21	126.5±1.6
1.43:1	31.6	30.3	32.3	122.3	129.1	127.8	31.4±1.01	126.4±3.6
2.5:1	33.0	32.3	32.8	133.4	128.8	127.5	32.7±0.36	129.9±3.1
10:1	31.0	32.2	31.0	128.9	126.7	126.4	31.4±0.69	127.3±1.4
20:1	33.2	32.9	31.5	124.4	126.3	128.2	32.5±0.91	126.3±1.9
30:1	31.4	32.8	32.0	129.1	129.0	131.0	32.1±0.70	129.7±1.1
40:1	30.5	30.7	32.3	132.7	138.3	135.9	31.2±0.99	135.6±2.8
50:1	31.7	31.5	31.2	141.2	149.2	142.2	31.5±0.25	144.2±4.4
60:1	19.4	20.1	19.9	865.3	665.2	1088	19.8±0.36	872.8±212
70:1	16.2	16.6	17.4	215.2	484.2	1268	16.7±0.61	655.7±547
80:1	19.8	20.6	20.5	1670	556.9	862.4	20.3±0.44	1030±575
90:1	21.5	22.7	22.4	2883	1521	884.2	22.2±0.62	1763±1021
100:1	26.7	26.4	26.6	1270	2287	2170	26.6±0.15	1909±556

Table A.2

Zeta Potential and Size Measurements for Varying SiO_2-PLL to Humic Acid Ratios

Ratio	Zeta potential (mV)			Particle size (nm)			Average	
	Prep 1	Prep 2	Prep 3	Prep 1	Prep 2	Prep 3	Zeta (mV)	Size (nm)
1:6	-10.5	-12.6	-10.9	2324	2229	2193	-11.3±1.12	2249±68
1:5	-11.6	-9.9	-10.4	2271	2560	1800	-10.6±0.87	2210±384
1:4	-29.3	-27.1	-30.7	881.6	809.9	870.4	-29.0±1.81	854.0±38.6
1:3	-33.4	-33.1	-29.6	209.1	207.2	207.7	-32.0±2.11	208.0±1.0
1:2	-13.9	-15.9	-13.9	2441	1083	2099	-14.6±1.15	1874±706
1:1	0.018	0.162	0.055	5170	4991	5399	0.078±0.07	5187±205
2:1	23.6	24.5	23.9	2889	3299	3201	24.0±0.46	3130±214
3:1	29.5	30.3	30.0	1190	980.0	1001	29.9±0.40	1057±116
4:1	30.2	28.7	29.2	325.4	451.4	381.4	29.4±0.76	386.1±63.1
5:1	27.2	29.1	27.8	1137	1098	1191	28.0±0.97	1142±47

Table A.3

Raw Fluorimeter Results: Calibration Data for Analysis of BaP on Humic Acid Coated Nanospheres

Elapsed time	Benzo[a]pyrene standard concentration				
	1 μg/L	2 μg/L	3 μg/L	4 μg/L	5 μg/L
24 hr	242856	471263	832284	1050501	1263291
48 hr	237438	538794	726501	911210	1230751
72 hr	235884	501685	798421	941969	1265404
96 hr	239924	490084	745157	951919	1116816
120 hr	245651	541816	804664	1168516	1304981
144 hr	249684	519815	861516	1268169	1268461
168 hr	233865	487535	856816	975117	1184618

Table A.4

Raw Fluorimeter Results: Sample Analysis of BaP on Humic Acid Coated Nanospheres

	Particle concentration				
Elapsed time	0.00 mg/L	0.01 mg/L	0.10 mg/L	0.50 mg/L	1.00 mg/L
24 hr	403785	429545	437159	404139	415780
48 hr	372660	394274	448851	376679	424461
72 hr	401517	418062	447882	412341	472543
96 hr	409849	400743	466295	398312	455449
120 hr	428778	455213	489621	431098	479335
144 hr	443084	431782	520431	459802	508182
168 hr	419401	434350	465777	409372	483970

Table A.5

Benzo[a]pyrene Concentration (µg/L) with Varying Amounts of Humic Acid Coated Nanospheres

	Particle concentration				
Elapsed time	0.00 mg/L	0.01 mg/L	0.10 mg/L	0.50 mg/L	1.00 mg/L
24 hr	1.595	1.693	1.722	1.596	1.640
48 hr	1.490	1.581	1.813	1.507	1.709
72 hr	1.611	1.677	1.797	1.654	1.895
96 hr	1.651	1.610	1.906	1.599	1.857
120 hr	1.600	1.696	1.822	1.608	1.784
144 hr	1.599	1.558	1.876	1.659	1.832
168 hr	1.626	1.689	1.820	1.584	1.897

Table A.6

Raw Fluorimeter Results: Calibration Data for Analysis of BaP Removed by SUVs Under SUV Standard Set 1 (50 mg/L)

	Benzo[a]pyrene standard concentration				
Elapsed time	1 μg/L	2 μg/L	3 μg/L	4 μg/L	5 μg/L
24 hr	364709	632931	907803	1185605	1453025
48 hr	400651	665108	965015	1268415	1519160
72 hr	356684	610098	941517	1068417	1508404
96 hr	336810	661087	919806	1196846	1448081
120 hr	401981	694093	1006468	1281682	1496406
144 hr	380511	651064	965153	1164318	1536810
168 hr	398132	662684	948110	1271980	1528640

Table A.7

Raw Fluorimeter Results: Calibration Data for Analysis of BaP Removed by SUVs Under SUV Standard Set 2 (100 mg/L)

	Benzo[a]pyrene standard concentration				
Elapsed time	1 μg/L	2 μg/L	3 μg/L	4 μg/L	5 μg/L
24 hr	467940	728964	978978	1230065	1466525
48 hr	426344	686540	978006	1268046	1410740
72 hr	464550	754216	932801	1196840	1468540
96 hr	493516	795604	1196403	1298450	1496708
120 hr	453267	735404	968407	1240840	1520332
144 hr	436810	706049	954164	1180696	1498228
168 hr	475998	800863	995404	1280351	1436077

Table A.8

Raw Fluorimeter Results: Individual Results for Sample Analysis of BaP Removed by SUVs from Humic Acid Coated Nanospheres

	Containing 50 mg/L of SUVs		
Elapsed time	Prep 1	Prep 2	Prep 3
24 hr	499548	560366	433752
48 hr	476456	579328	439539
72 hr	524512	544060	418801
96 hr	525927	513036	337932
120 hr	610793	641681	527635
144 hr	552340	614980	495479
168 hr	592122	619814	530937
	Containing 100 mg/L of SUVs		
Elapsed time	Prep 1	Prep 2	Prep 3
24 hr	488170	379398	485962
48 hr	533565	480008	539677
72 hr	518527	483483	532495
96 hr	620888	621642	675135
120 hr	557276	531088	536203
144 hr	556601	557363	561714
168 hr	615827	654222	630153
	Containing 1000 mg/L of SUVs, diluted to 50 mg/L		
Elapsed time	Prep 1	Prep 2	Prep 3
24 hr	158516	130719	120356
48 hr	168154	150113	145204
72 hr	113629	108330	93584
96 hr	131716	122003	114023
120 hr	193195	172084	170293
	Containing 1000 mg/L of SUVs, diluted to 100 mg/L		
Elapsed time	Prep 1	Prep 2	Prep 3
24 hr	295002	286323	287548
48 hr	260786	237105	246942
72 hr	295136	279387	288122
96 hr	381175	363187	356478
120 hr	270730	259221	244933

Table A.9

Individual Calculated Results for Sample Analysis of BaP Removed by SUVs from Humic Acid Coated Nanospheres

	Containing 50 mg/L of SUVs		
Elapsed time	Prep 1	Prep 2	Prep 3
24 hr	1.500	1.723	1.259
48 hr	1.285	1.647	1.155
72 hr	1.651	1.722	1.268
96 hr	1.598	1.552	0.917
120 hr	1.684	1.795	1.385
144 hr	1.630	1.851	1.428
168 hr	1.712	1.808	1.499
	Containing 100 mg/L of SUVs		
Elapsed time	Prep 1	Prep 2	Prep 3
24 hr	1.053	0.618	1.045
48 hr	1.352	1.142	1.376
72 hr	1.185	1.042	1.242
96 hr	1.265	1.268	1.482
120 hr	1.385	1.285	1.305
144 hr	1.465	1.468	1.485
168 hr	1.408	1.568	1.468
	Containing 1000 mg/L of SUVs, diluted to 50 mg/L		
Elapsed time	Prep 1	Prep 2	Prep 3
24 hr	5.019	2.982	2.223
48 hr	3.984	2.714	2.368
72 hr	3.268	2.885	1.817
96 hr	3.385	2.680	2.102
120 hr	3.602	2.081	1.952
	Containing 1000 mg/L of SUVs, diluted to 100 mg/L		
Elapsed time	Prep 1	Prep 2	Prep 3
24 hr	2.801	2.454	2.503
48 hr	2.821	1.892	2.278
72 hr	2.731	2.088	2.445
96 hr	3.101	2.384	2.117
120 hr	2.991	2.555	2.014

Table A.10

Average Benzo[a]pyrene Removed by SUVs from Humic Acid-Coated Nanospheres

	Concentration of SUVs			
Elapsed time	50 mg/L	100 mg/L	1000 mg/L *diluted to 50 mg/L*	1000 mg/L *diluted to 100 mg/L*
24 hr	1.494±0.232	0.905±0.249	3.408±1.446	2.586±0.188
48 hr	1.362±0.255	1.290±0.129	3.022±0.851	2.330±0.466
72 hr	1.547±0.244	1.156±0.103	2.657±0.752	2.421±0.322
96 hr	1.356±0.381	1.338±0.124	2.722±0.642	2.534±0.509
120 hr	1.621±0.212	1.325±0.053	2.545±0.918	2.520±0.490
144 hr	1.637±0.212	1.473±0.011	N/A	N/A
168 hr	1.673±0.158	1.482±0.081	N/A	N/A